

# Final Results of the GEp-III Experiment (E04-108)

Andrew Puckett

Los Alamos National Laboratory

on behalf of the GEp-III Collaboration

4th Workshop on Exclusive Reactions at

High Momentum Transfer

Jefferson Lab

5/19/2010

# Outline

- Nucleon form factors overview
- Experiments E04-108 and E04-019 overview
- Data analysis
- Results
  - E04-108 final results (~~submitted to~~ accepted by PRL)
- Statistical Impact of E04-108 results
- Conclusion

# GEp-III Collaboration

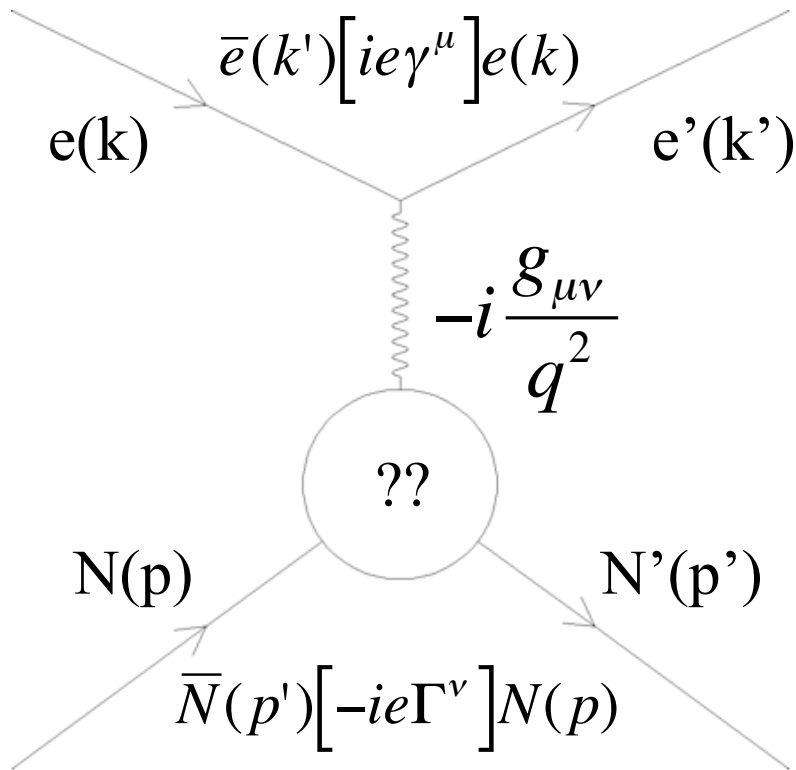
## Recoil Polarization Measurements of the Proton Electromagnetic Form Factor Ratio to $Q^2 = 8.5 \text{ GeV}^2$

A. J. R. Puckett,<sup>1,\*</sup> E. J. Brash,<sup>2,3</sup> M. K. Jones,<sup>3</sup> W. Luo,<sup>4</sup> M. Meziane,<sup>5</sup> L. Pentchev,<sup>5</sup> C. F. Perdrisat,<sup>5</sup> V. Punjabi,<sup>6</sup> F. R. Wesselmann,<sup>6</sup> A. Ahmidouch,<sup>7</sup> I. Albayrak,<sup>8</sup> K. A. Aniol,<sup>9</sup> J. Arrington,<sup>10</sup> A. Asaturyan,<sup>11</sup> H. Baghdasaryan,<sup>12</sup> F. Benmokhtar,<sup>13</sup> W. Bertozzi,<sup>1</sup> L. Bimbot,<sup>14</sup> P. Bosted,<sup>3</sup> W. Boeglin,<sup>15</sup> C. Butuceanu,<sup>16</sup> P. Carter,<sup>2</sup> S. Chernenko,<sup>17</sup> E. Christy,<sup>8</sup> M. Comisso,<sup>12</sup> J. C. Cornejo,<sup>9</sup> S. Covrig,<sup>3</sup> S. Danagoulian,<sup>7</sup> A. Daniel,<sup>18</sup> A. Davidenko,<sup>19</sup> D. Day,<sup>12</sup> S. Dhamija,<sup>15</sup> D. Dutta,<sup>20</sup> R. Ent,<sup>3</sup> S. Frullani,<sup>21</sup> H. Fenker,<sup>3</sup> E. Frlez,<sup>12</sup> F. Garibaldi,<sup>21</sup> D. Gaskell,<sup>3</sup> S. Gilad,<sup>1</sup> R. Gilman,<sup>3,22</sup> Y. Goncharenko,<sup>19</sup> K. Hafidi,<sup>10</sup> D. Hamilton,<sup>23</sup> D. W. Higinbotham,<sup>3</sup> W. Hinton,<sup>6</sup> T. Horn,<sup>3</sup> B. Hu,<sup>4</sup> J. Huang,<sup>1</sup> G. M. Huber,<sup>16</sup> E. Jensen,<sup>2</sup> C. Keppel,<sup>8</sup> M. Khandaker,<sup>6</sup> P. King,<sup>18</sup> D. Kirillov,<sup>17</sup> M. Kohl,<sup>8</sup> V. Kravtsov,<sup>19</sup> G. Kumbartzki,<sup>22</sup> Y. Li,<sup>8</sup> V. Mamyran,<sup>12</sup> D. J. Margaziotis,<sup>9</sup> A. Marsh,<sup>2</sup> Y. Matulenko,<sup>19</sup> J. Maxwell,<sup>12</sup> G. Mbianda,<sup>24</sup> D. Meekins,<sup>3</sup> Y. Melnik,<sup>19</sup> J. Miller,<sup>25</sup> A. Mkrtchyan,<sup>11</sup> H. Mkrtchyan,<sup>11</sup> B. Moffit,<sup>1</sup> O. Moreno,<sup>9</sup> J. Mulholland,<sup>12</sup> A. Narayan,<sup>20</sup> S. Nedev,<sup>26</sup> Nuruzzaman,<sup>20</sup> E. Piasetzky,<sup>27</sup> W. Pierce,<sup>2</sup> N. M. Piskunov,<sup>17</sup> Y. Prok,<sup>2</sup> R. D. Ransome,<sup>22</sup> D. S. Razin,<sup>17</sup> P. Reimer,<sup>10</sup> J. Reinhold,<sup>15</sup> O. Rondon,<sup>12</sup> M. Shabestari,<sup>12</sup> A. Shahinyan,<sup>11</sup> K. Shestermanov,<sup>19,†</sup> S. Širca,<sup>28</sup> I. Sitnik,<sup>17</sup> L. Smykov,<sup>17,†</sup> G. Smith,<sup>3</sup> L. Solovyev,<sup>19</sup> P. Solvignon,<sup>10</sup> R. Subedi,<sup>12</sup> E. Tomasi-Gustafsson,<sup>14,29</sup> A. Vasiliev,<sup>19</sup> M. Veilleux,<sup>2</sup> B. B. Wojtsekhowski,<sup>3</sup> S. Wood,<sup>3</sup> Z. Ye,<sup>8</sup> Y. Zanevsky,<sup>17</sup> X. Zhang,<sup>4</sup> Y. Zhang,<sup>4</sup> X. Zheng,<sup>12</sup> and L. Zhu<sup>1</sup>

# Institutions

- <sup>1</sup>Massachusetts Institute of Technology, Cambridge, MA 02139  
<sup>2</sup>Christopher Newport University, Newport News, VA 23606  
<sup>3</sup>Thomas Jefferson National Accelerator Facility, Newport News, VA 23606  
<sup>4</sup>Lanzhou University, Lanzhou 730000, Gansu, Peoples Republic of China  
<sup>5</sup>College of William and Mary, Williamsburg, VA 23187  
<sup>6</sup>Norfolk State University, Norfolk, VA 23504  
<sup>7</sup>North Carolina A&T State University, Greensboro, NC 27411  
<sup>8</sup>Hampton University, Hampton, VA 23668  
<sup>9</sup>California State University Los Angeles, Los Angeles, CA 90032  
<sup>10</sup>Argonne National Laboratory, Argonne, IL, 60439  
<sup>11</sup>Yerevan Physics Institute, Yerevan 375036, Armenia  
<sup>12</sup>University of Virginia, Charlottesville, VA 22904  
<sup>13</sup>Carnegie Mellon University, Pittsburgh, PA 15213  
<sup>14</sup>Institut de Physique Nucléaire, CNRS/IN2P3 and Université Paris-Sud, France  
<sup>15</sup>Florida International University, Miami, FL 33199  
<sup>16</sup>University of Regina, Regina, SK S4S 0A2, Canada  
<sup>17</sup>JINR-LHE, Dubna, Moscow Region, Russia 141980  
<sup>18</sup>Ohio University, Athens, Ohio 45701  
<sup>19</sup>IHEP, Protvino, Moscow Region, Russia 142284  
<sup>20</sup>Mississippi State University, Mississippi, MS 39762  
<sup>21</sup>INFN, Sezione Sanità and Istituto Superiore di Sanità, 00161 Rome, Italy  
<sup>22</sup>Rutgers, The State University of New Jersey, Piscataway, NJ 08855  
<sup>23</sup>University of Glasgow, Glasgow G12 8QQ, Scotland UK  
<sup>24</sup>University of Witwatersrand, Johannesburg, South Africa  
<sup>25</sup>University of Maryland, College Park, MD 20742  
<sup>26</sup>University of Chemical Technology and Metallurgy, Sofia, Bulgaria  
<sup>27</sup>University of Tel Aviv, Tel Aviv, Israel  
<sup>28</sup>University of Ljubljana, SI-1000 Ljubljana, Slovenia  
<sup>29</sup>DSM, IRFU, SPhN, Saclay, 91191 Gif-sur-Yvette, France

# Overview of Nucleon Form Factors



**One-photon exchange (OPEX)  
mechanism for elastic  $eN$   
scattering**

Definitions and Formulas:

$$\Gamma^\mu = F_1(q^2)\gamma^\mu + F_2(q^2)\frac{i\sigma^{\mu\nu}q_\nu}{2M}$$

$$Q^2 = -q^2 > 0$$

$$G_E = F_1 - \tau F_2$$

$$G_M = F_1 + F_2$$

$$\tau \equiv \frac{Q^2}{4M^2}$$

$$\frac{d\sigma}{d\Omega_e} = \frac{\alpha^2}{Q^2} \left( \frac{E'_e}{E_e} \right) \left[ \frac{G_E^2 + \tau G_M^2}{1 + \tau} \cot^2 \left( \frac{\theta_e}{2} \right) + 2\tau G_M^2 \right]$$

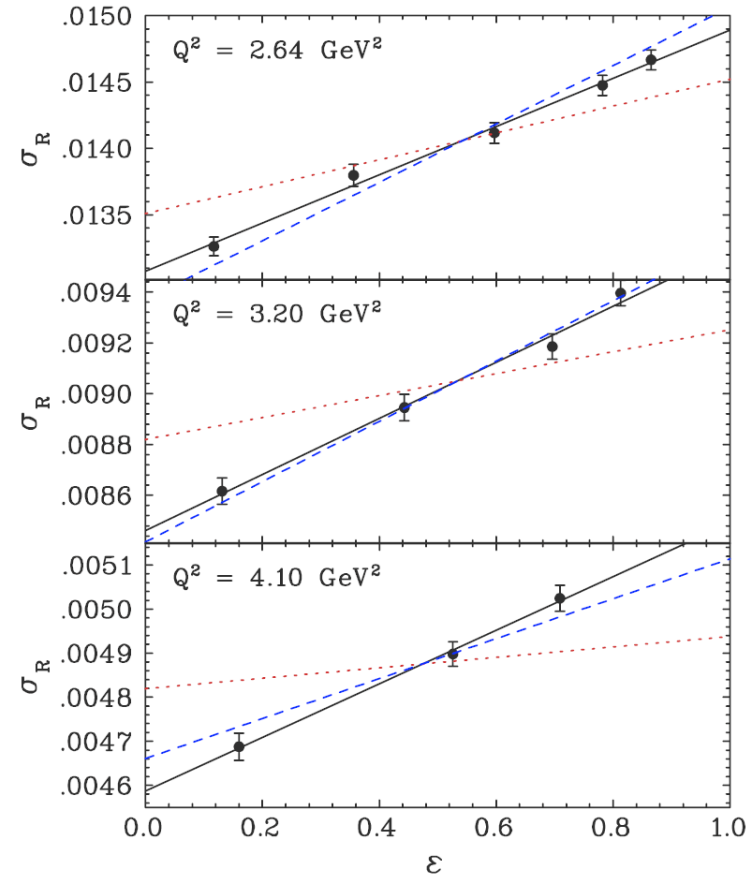
Lab Differential Cross Section:  
Rosenbluth Formula

# Rosenbluth (L/T) Separation

$$\sigma_r \equiv (1 + \tau) \varepsilon \frac{\sigma_{eN}}{\sigma_{Mott}} = \varepsilon G_E^2 + \tau G_M^2$$

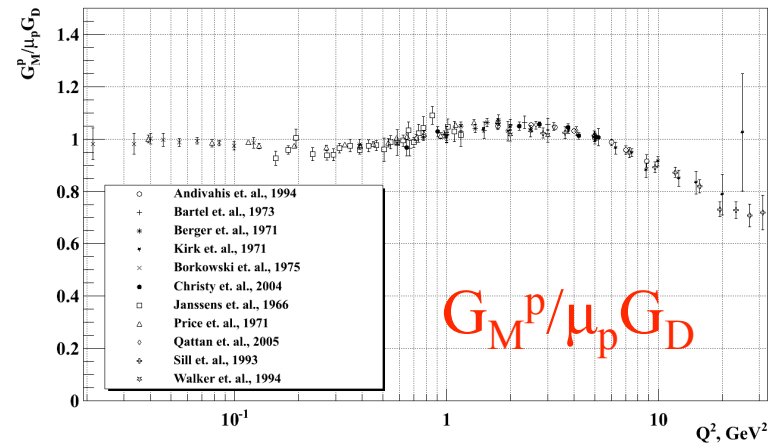
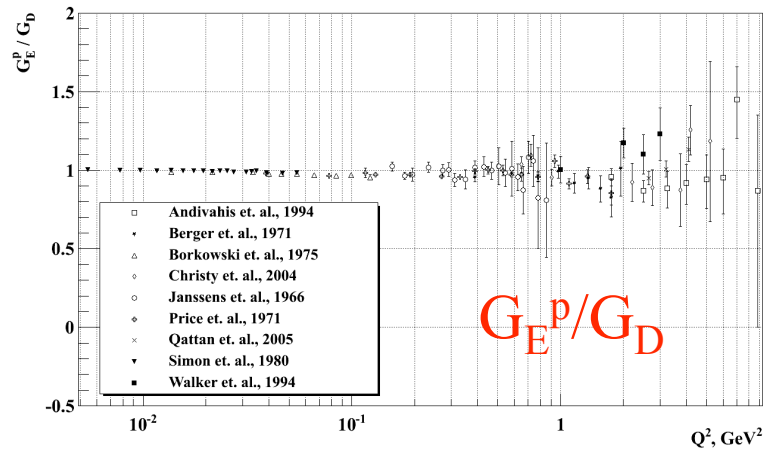
$$\varepsilon = \left[ 1 + 2(1 + \tau) \tan^2 \left( \frac{\theta_e}{2} \right) \right]^{-1}$$

- Measure angular dependence of scattering cross section at fixed  $Q^2$
- In OPEX, “reduced cross section” is linear in  $\varepsilon$
- Slope and intercept determine  $G_E^2$ ,  $G_M^2$  respectively



PRL 94, 142301 (2005)

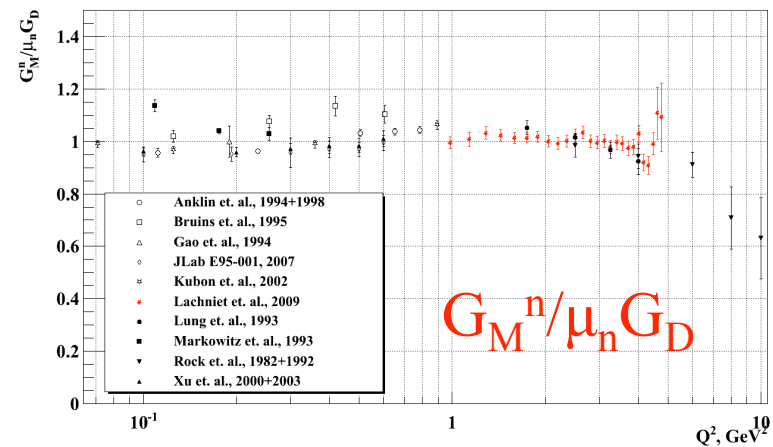
# World Cross-Section Data



- Cross section data for  $G_E^p$ ,  $G_M^p$ ,  $G_M^n$  qualitatively described by dipole form:

$$G_D = \left(1 + \frac{Q^2}{\Lambda^2}\right)^{-2} \quad \Lambda^2 = 0.71 \text{ GeV}^2$$

- L/T separation becomes insensitive to  $G_M(G_E)$  at small (large)  $Q^2$
- Method impractical for (small)  $G_E^n$



# Polarization Transfer

$$p(\vec{e}, e' \vec{p})$$

$$I_0 P_l = \sqrt{\tau(1+\tau)} \tan^2\left(\frac{\theta_e}{2}\right) \frac{E_e + E'_e}{M} G_M^2$$

$$I_0 P_t = -2\sqrt{\tau(1+\tau)} \tan\left(\frac{\theta_e}{2}\right) G_E G_M$$

$$P_n = 0$$

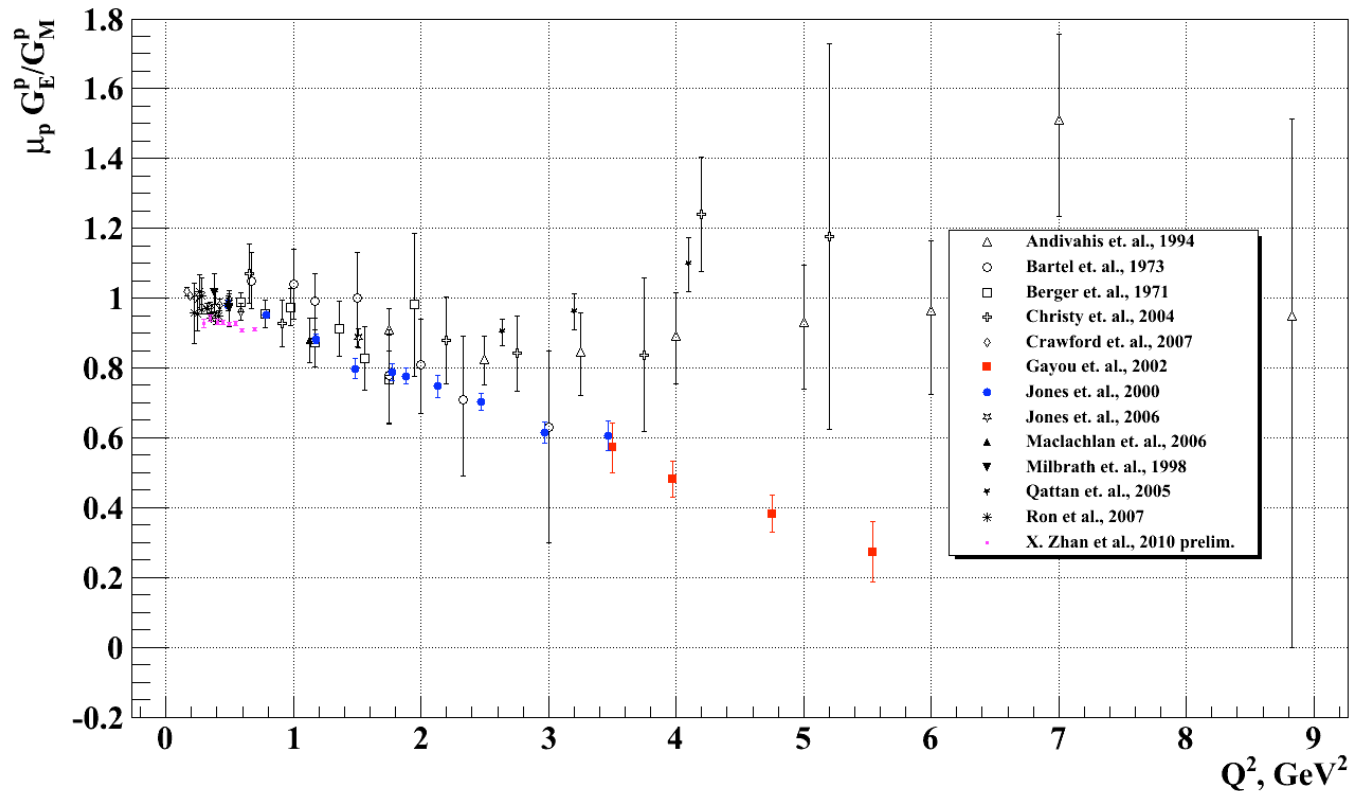
$$I_0 \equiv G_E^2 + \frac{\tau}{\varepsilon} G_M^2$$

$$\frac{G_E}{G_M} = -\frac{P_t}{P_l} \frac{E_e + E'_e}{2M} \tan\left(\frac{\theta_e}{2}\right)$$

- Elastic scattering of polarized electrons from unpolarized nucleons transfers polarization to scattered nucleons
- Better sensitivity to  $G_E$ , especially at high  $Q^2$
- Determines sign of  $G_E/G_M$
- Much lower sensitivity to radiative corrections and two-photon-exchange (TPEX) than cross section

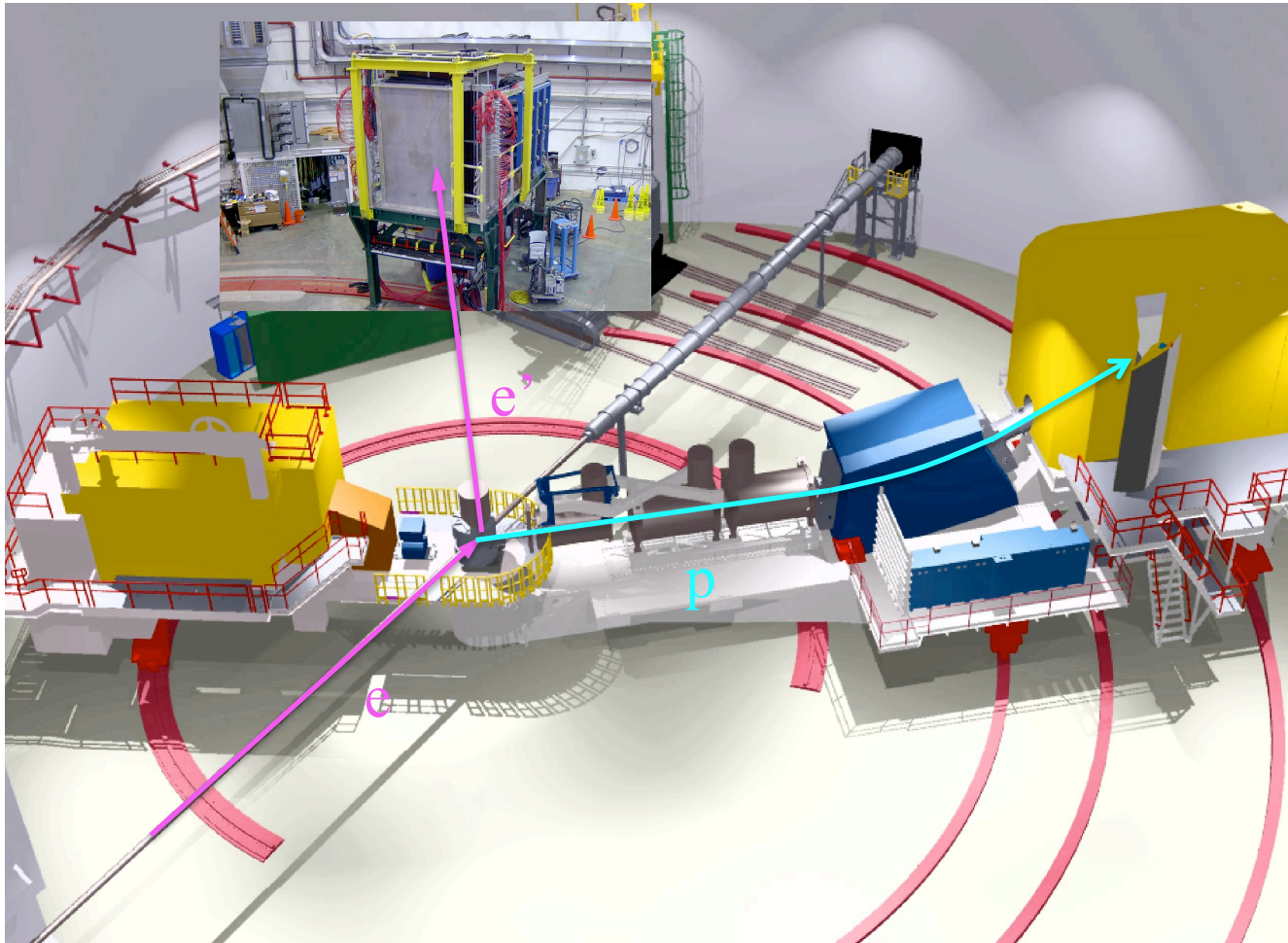


# Polarization Transfer and $G_E^p/G_M^p$



Precise recoil polarization data for  $R = \mu_p G_E^p / G_M^p$  conclusively revealed a strong deviation from  $R \approx 1$  scaling of cross section data

# Experiments E04-108 & E04-019



New recoil polarization measurements of  $G_E^p/G_M^p$  in Hall C at JLab

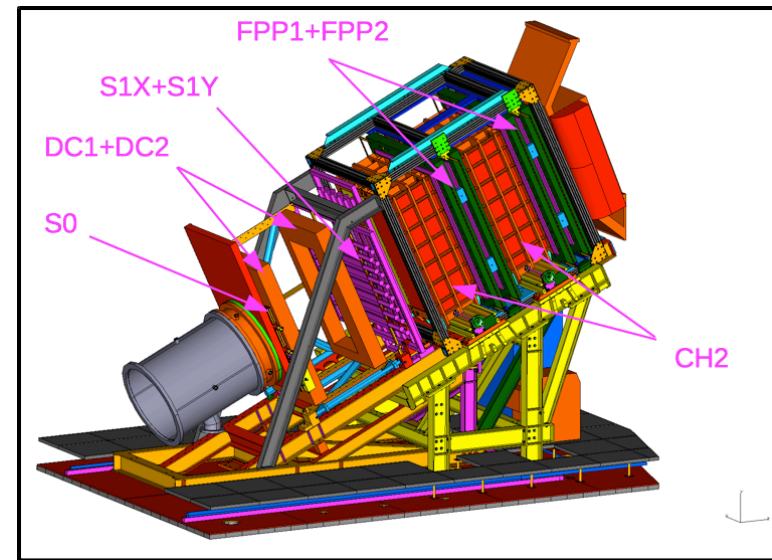
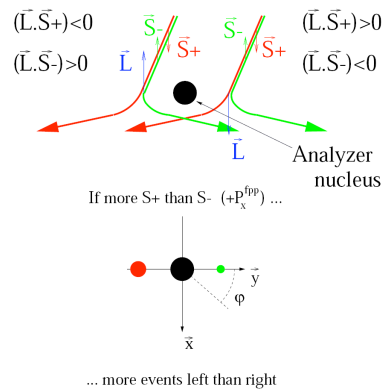
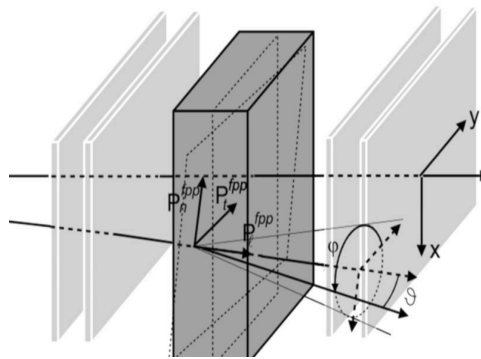
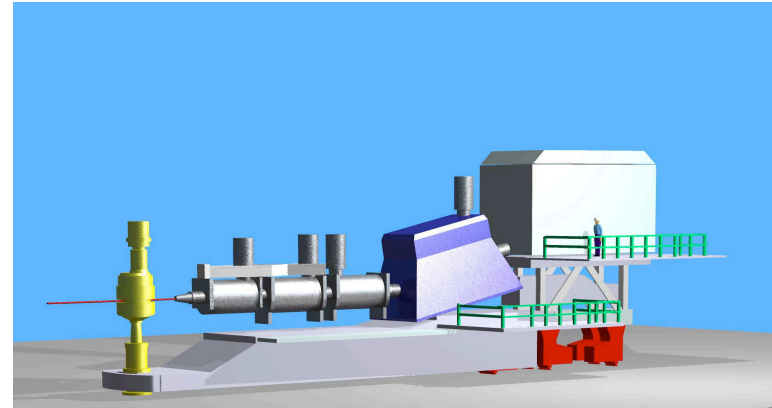
# Kinematics

$Q^2, \text{ GeV}^2$	$\varepsilon$	$E_{beam}, \text{ GeV}$	$\theta_p, ^\circ$	$p_p, \text{ GeV}$	$E_e, \text{ GeV}$	$\theta_e, ^\circ$
2.5	0.154	1.873	14.495	2.0676	0.532	105.2
2.5	0.633	2.847	30.985	2.0676	1.51	44.9
2.5	0.789	3.680	36.10	2.0676	2.37	30.8
5.2	0.377	4.053	17.94	3.5887	1.27	60.3
6.8	0.507	5.714	19.10	4.4644	2.10	44.2
8.5	0.236	5.714	11.6	5.407	1.16	69.0

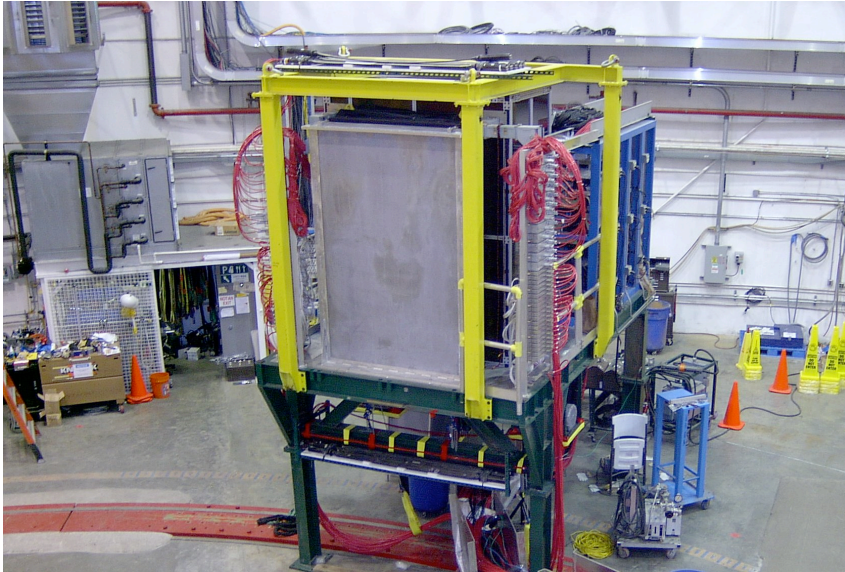
- E04-108: three new high  $Q^2$  measurements
- E04-019: precision measurements at  $Q^2=2.5 \text{ GeV}^2$  for three  $\varepsilon$  values; look for signatures of TPEX
- Beam:  $\sim 60\text{-}100 \mu\text{A}$  CW, 80-85% polarized (Moller)
- Target: 20 cm  $\text{LH}_2$ , nominal luminosity  $\sim 4 \times 10^{38} \text{ s}^{-1}\text{cm}^{-2}$

# HMS+FPP

- High Momentum Spectrometer (HMS), superconducting, 25° vertical bend magnetic spectrometer measures proton:
  - Angles
  - Momentum
  - Vertex
- Focal Plane Polarimeter:
  - Measure transverse components of proton polarization at the focal plane



# BigCal

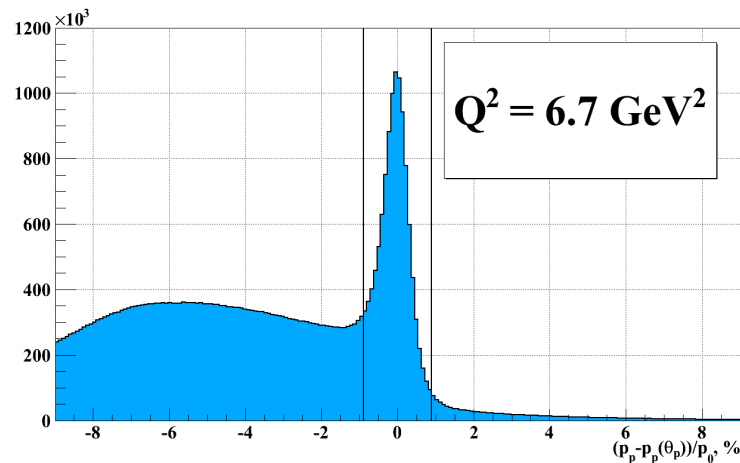
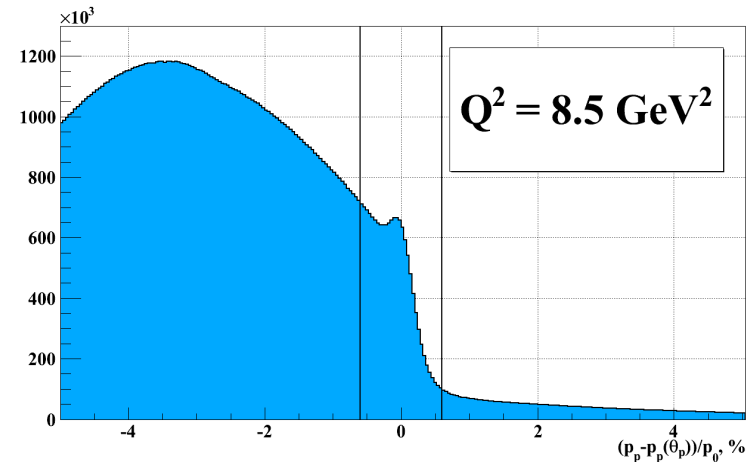
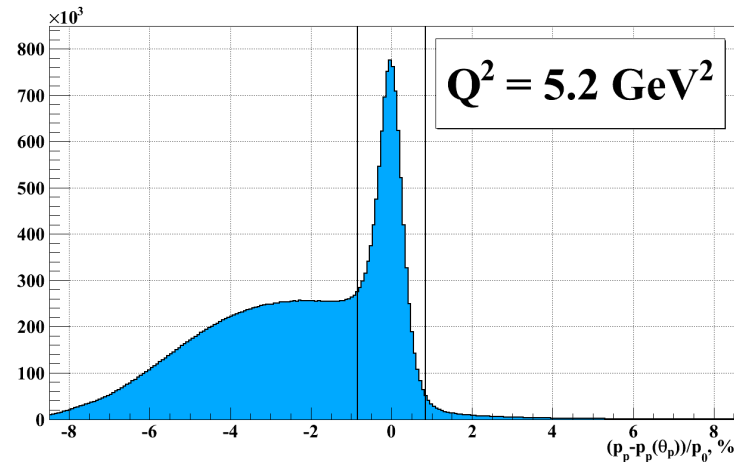


- Measure electron angles, energy
- Separate elastic from inelastic using angular correlation
- Large Jacobian in elastic ep scattering—large acceptance to match proton arm
- For  $Q^2 = 8.5 \text{ GeV}^2$ ,  $\Omega_e = 143 \text{ msr}$  to  $\Omega_p = 6.7 \text{ msr}$

# Data Analysis

- Elastic Event Selection
  - Inelasticity variable definitions
  - Cut selection and background estimation
- Extraction of Polarization Observables
  - Focal plane asymmetry extraction
  - Spin precession calculation

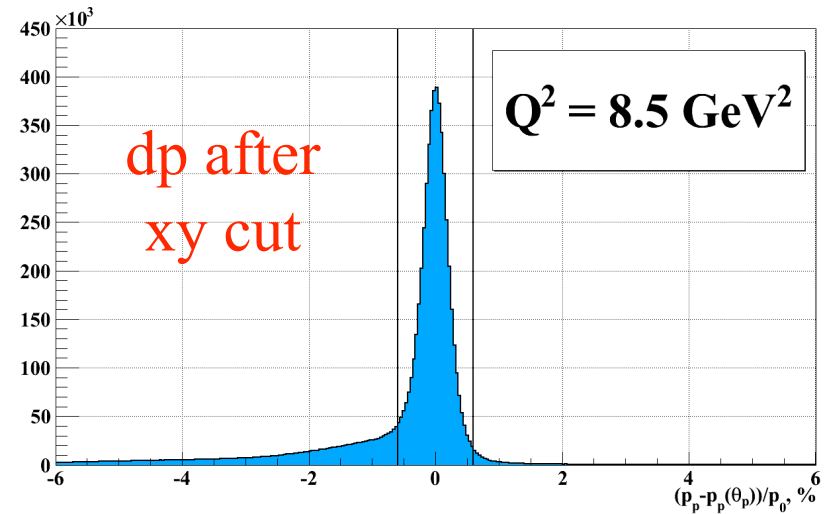
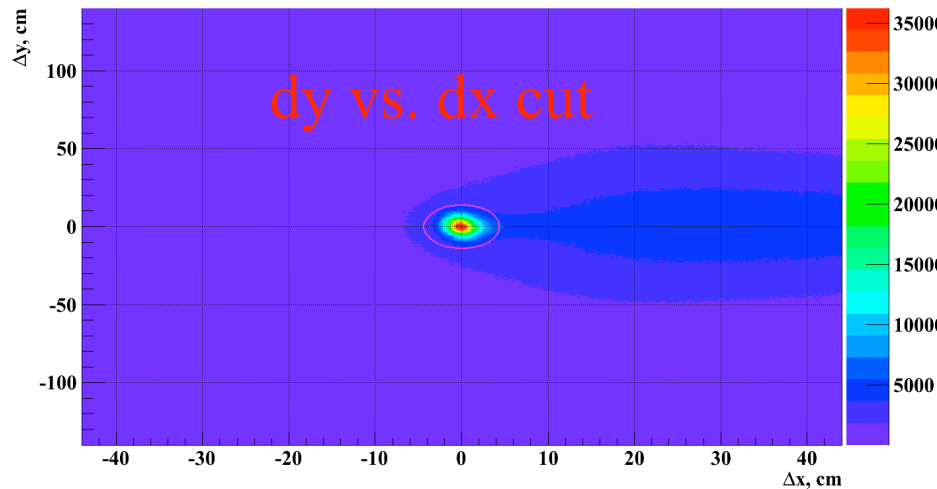
# Elastic Event Selection, I



$$p_p(\theta_p) = \frac{2M_p E_e (E_e + M_p) \cos \theta_p}{M_p^2 + 2M_p E_e + E_e^2 \sin^2 \theta_p}$$

- Proton angle-momentum correlation in elastic scattering
- $p$ - $p(\theta)$  spectra before applying cuts to BigCal electron position

# Elastic Event Selection, II

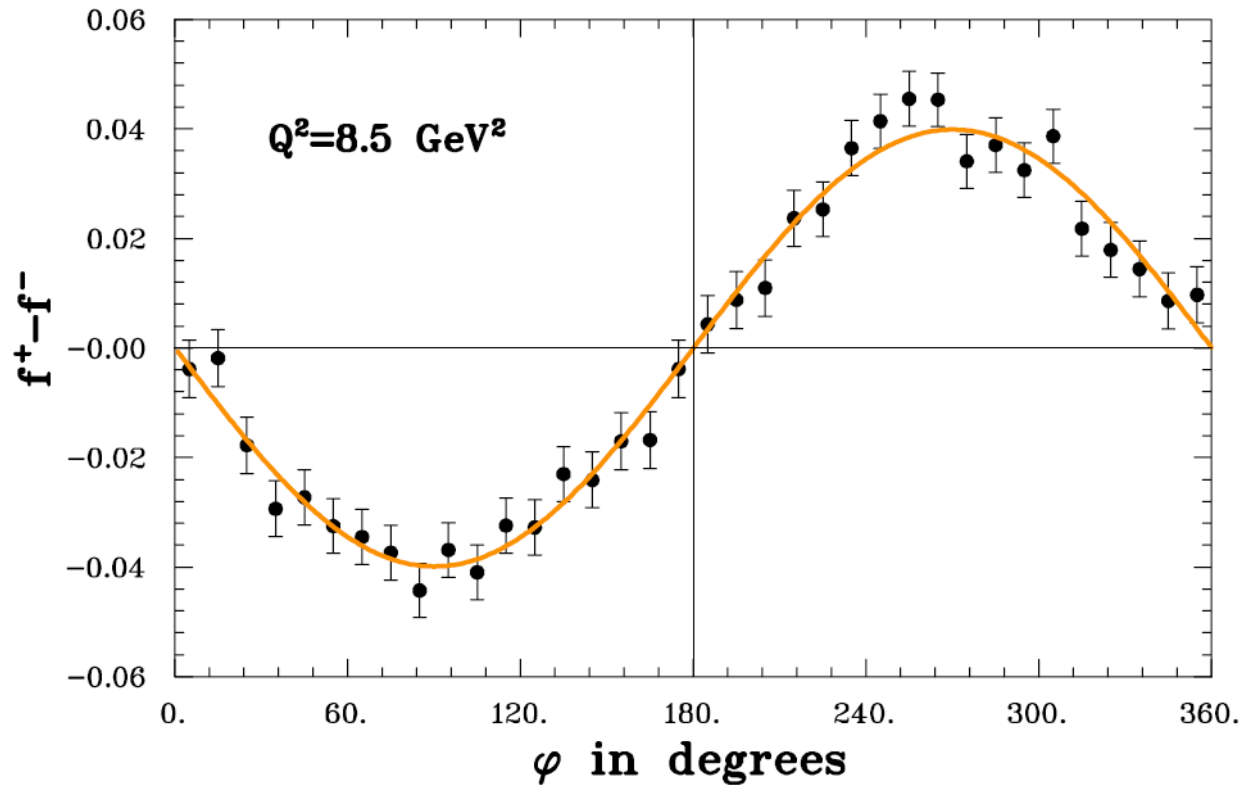


$$\left(\frac{\Delta x}{x_{\max}}\right)^2 + \left(\frac{\Delta y}{y_{\max}}\right)^2 \leq 1$$

- Elliptical cut at BigCal cleans up “dp” spectrum rather efficiently
- Fat tail on inelastic side of peak indicates “leftover” background
- Tight cuts to dx, dy, dp needed
- Still ~6% background for final cuts at  $Q^2=8.5 \text{ GeV}^2$



# Polarization Observables—FPP Asymmetry



$$f_+ - f_- = A \sin(\varphi + \delta)$$

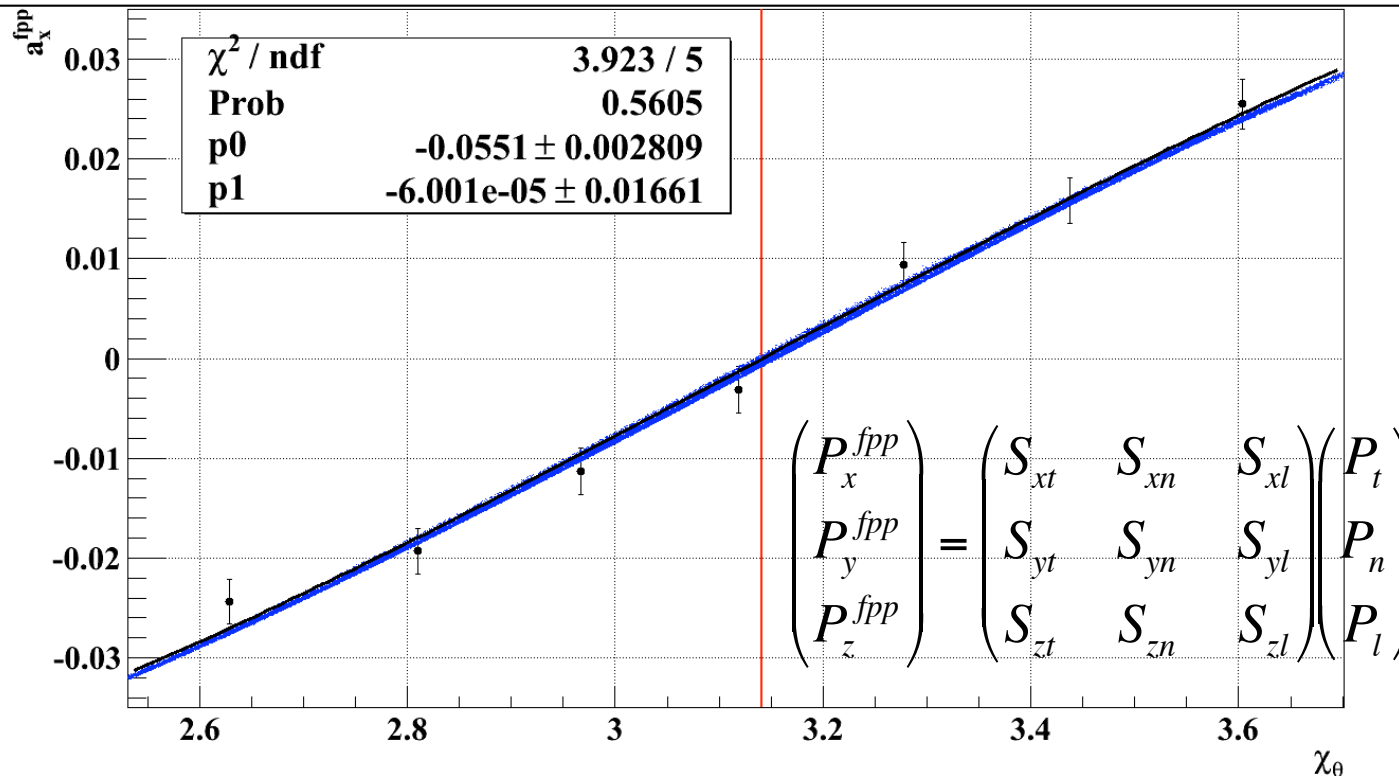
$$A = \overline{A}_y \sqrt{\left(P_x^{fpp}\right)^2 + \left(P_y^{fpp}\right)^2}$$

$$\tan \delta = -\frac{P_y^{fpp}}{P_x^{fpp}}$$

Helicity difference asymmetry,  $Q^2 = 8.5 \text{ GeV}^2$ ,  $0.5^\circ \leq \theta \leq 14.0^\circ$

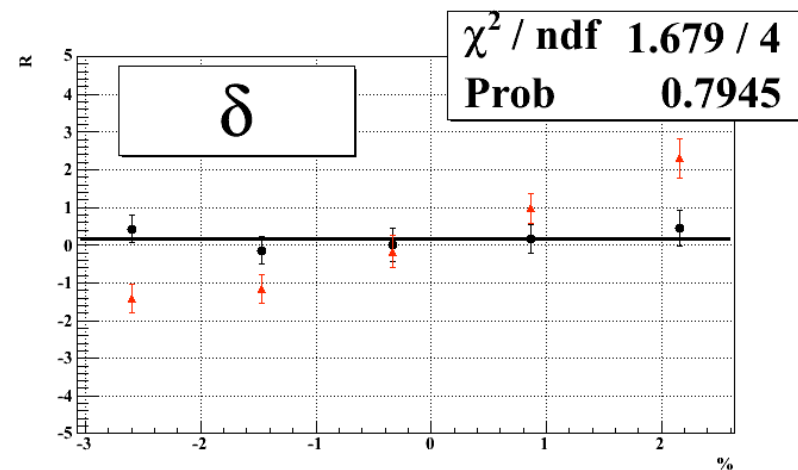
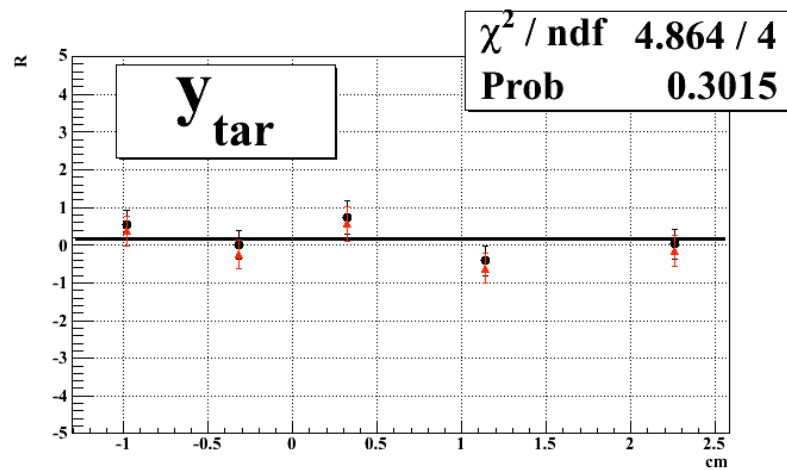
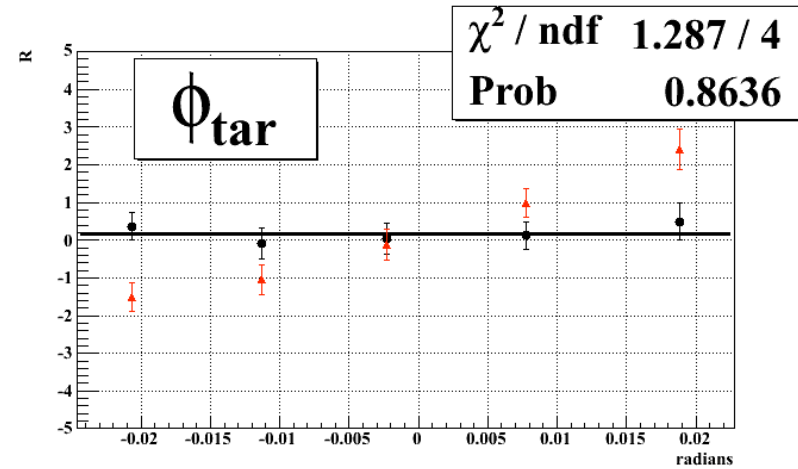
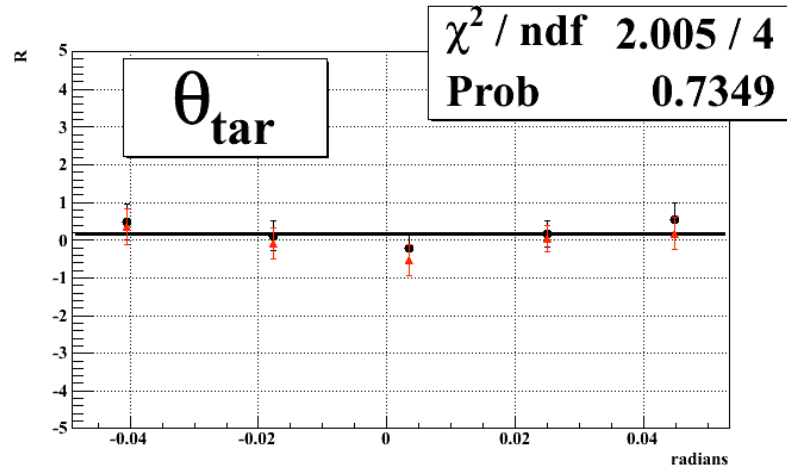
# Spin Precession, I

$Q^2=5.2 \text{ GeV}^2$ , zero crossing =  $180^\circ$  -  $p1 = (180.00 \pm 0.95)^\circ$



- Normal asymmetry at focal plane should cross zero at  $\chi=180^\circ$
- Within statistics, data compatible with this prediction
- Fit:  $a_x = p0 \sin(\chi+p1)$ ,  $\langle hA_y \rangle S_{xt} P_l$  from COSY agrees with  $\chi$ -dependence of the data

# Spin Precession, II



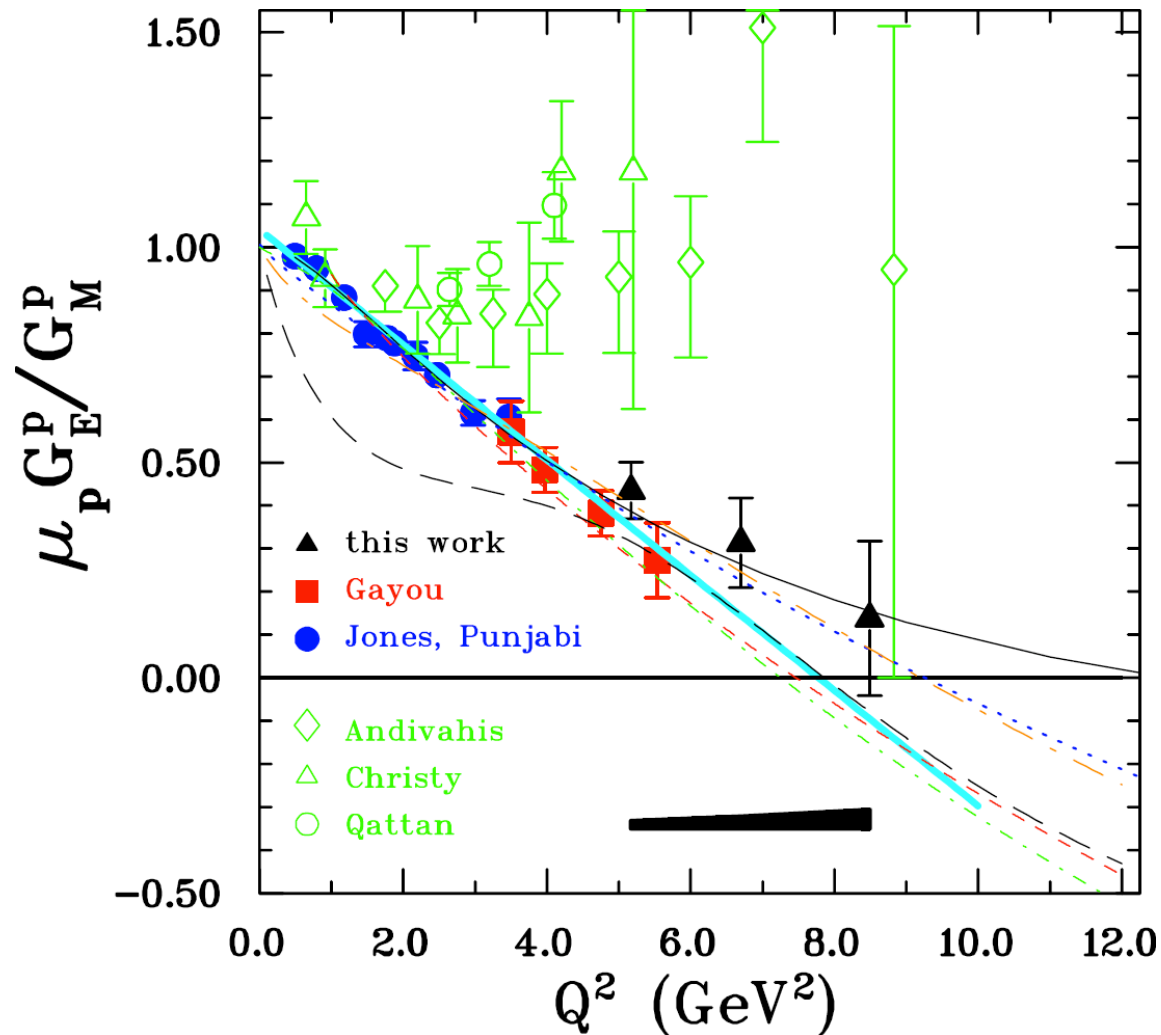
R vs. reconstructed kinematics,  $Q^2 = 8.5 \text{ GeV}^2$ , **DIPOLE/COSY**

# Systematic Uncertainties

$Q^2$ , GeV <sup>2</sup>	5.2	6.7	8.5
$\phi_{\text{bend}} (\pm 0.5 \text{ mrad})$	.0162	.0202	.0378
$\theta_{\text{bend}} (\pm 2 \text{ mrad})$	.0009	.0006	.0002
$\delta (\pm 0.3\%)$	.0029	.0027	.0024
$\varphi_{\text{fpp}} (\pm 0.14 \text{ mrad}/\sin(\vartheta_{\text{fpp}}))$	.0003	.0057	.0178
$E_{\text{beam}} (\pm 0.05\%)$	.00027	.00009	.00025
False asym.	.0069	.0057	.0018
Background	.0015	.0013	.0130
Rad. Corr. (% of R)	0.05% ( $\Delta R \approx -0.0002$ )	0.12% ( $\Delta R \approx -0.0004$ )	0.13% ( $\Delta R \approx -0.0002$ )
<b>Total <math>\Delta R_{\text{syst}}</math></b>	<b>.018</b>	<b>.022</b>	<b>.043</b>

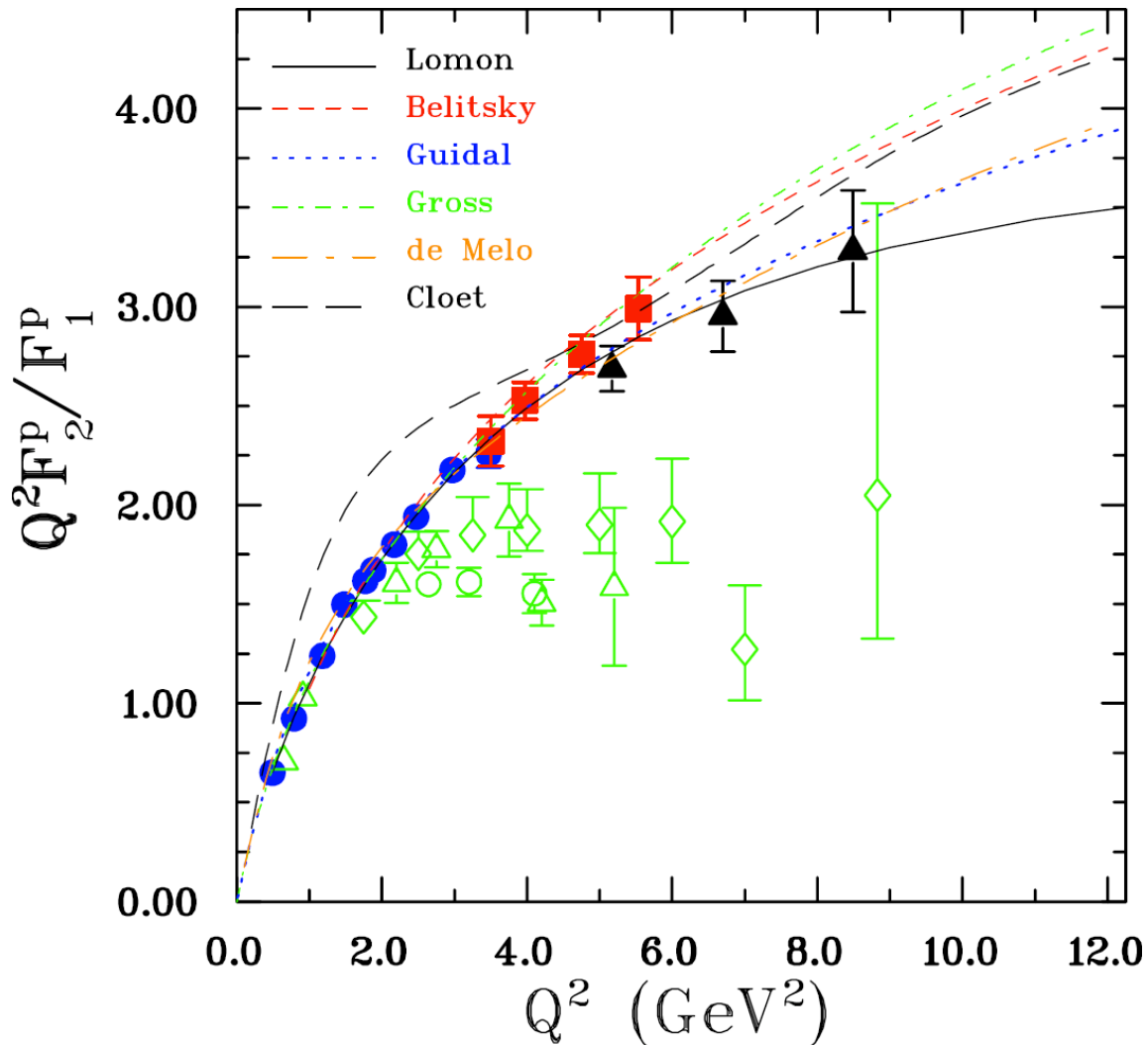
- Non-dispersive precession uncertainty dominates the systematic uncertainty in R
- $A_y$ ,  $h$  cancel, no uncertainty for R
- Standard radiative corrections (not applied) **negligible** compared to other uncertainties

# Final Results, I



- Results finalized, accepted for publication in PRL
- 50% increase in  $Q^2$  coverage
- New data favor a slowing rate of decrease of R

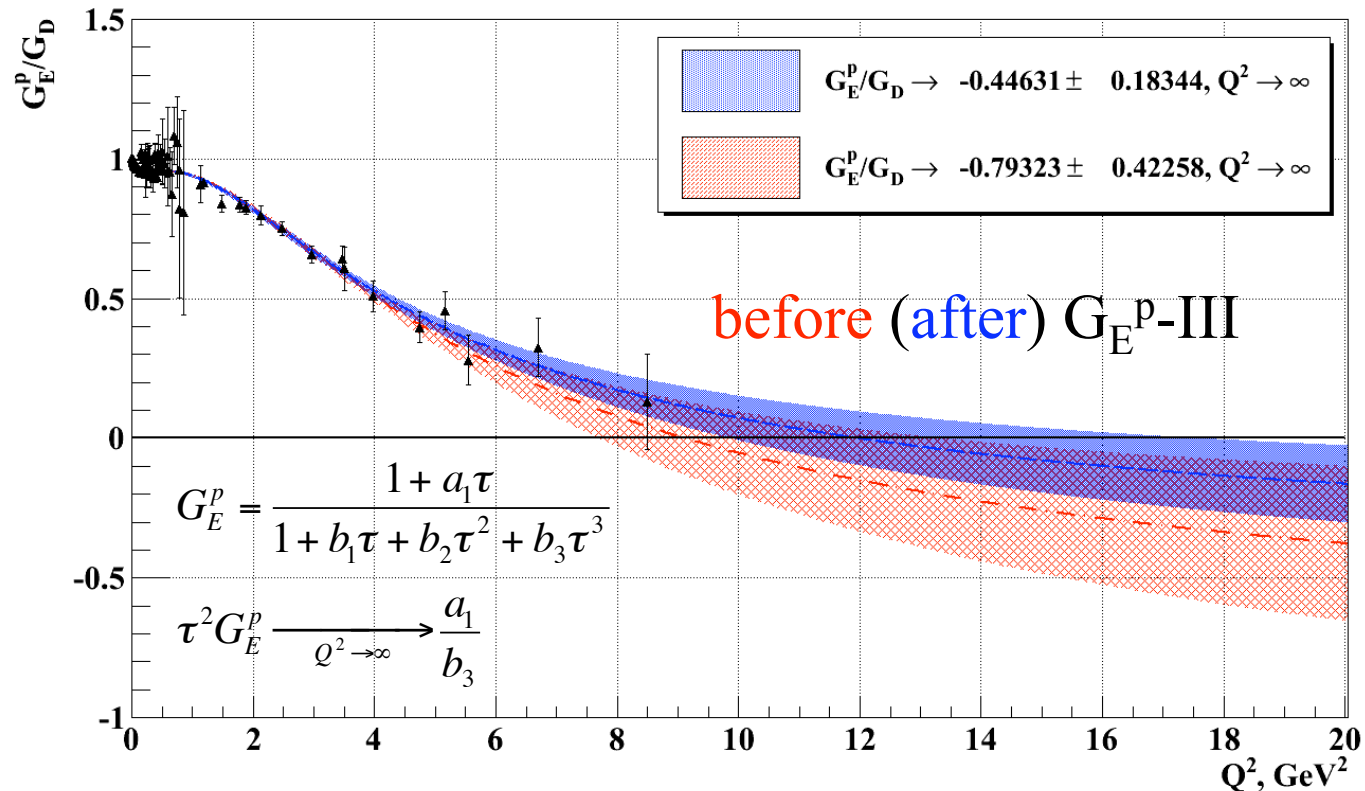
# Final Results, II



## • Theory curves:

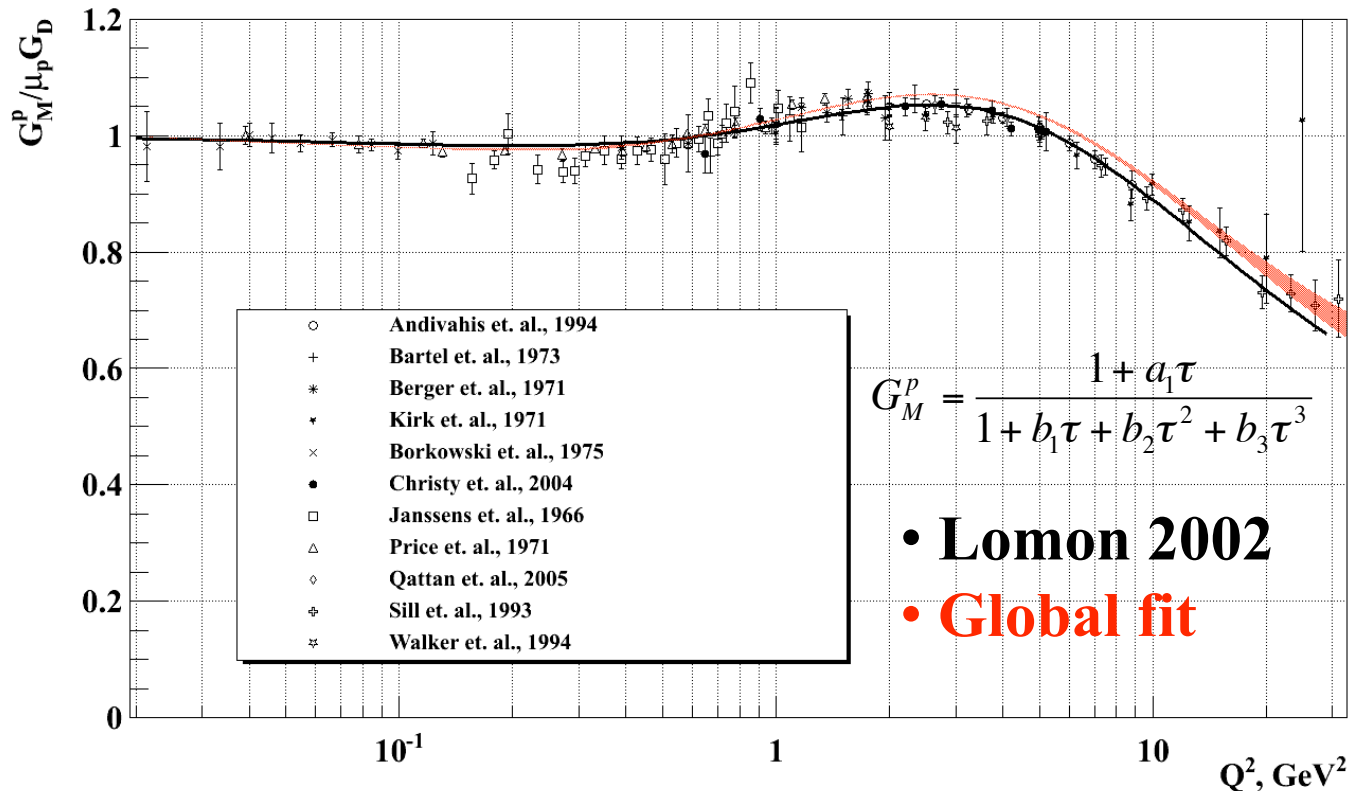
- Lomon 2002, 2006 (VMD)
- Belitsky 2003 (pQCD scaling)
- Guidal 2005 (GPD)
- Gross 2006, 2008 (covariant spectator model)
- de Melo 2009 (Bethe-Salpeter Amplitude)
- Cloet 2009 (Dyson-Schwinger/Faddeev/quark-diquark)

# Statistical Impact of GEp-III



- Global fit of  $G_E^p$  and  $G_M^p$  using Kelly parametrization: PRC 70, 068202 (2004)
- Including GEp-III data pushes zero crossing from  $\sim 9$  to  $\sim 12 \text{ GeV}^2$ , reduces uncertainty in asymptotic  $G_E^p/G_D$  by a factor of more than 2.

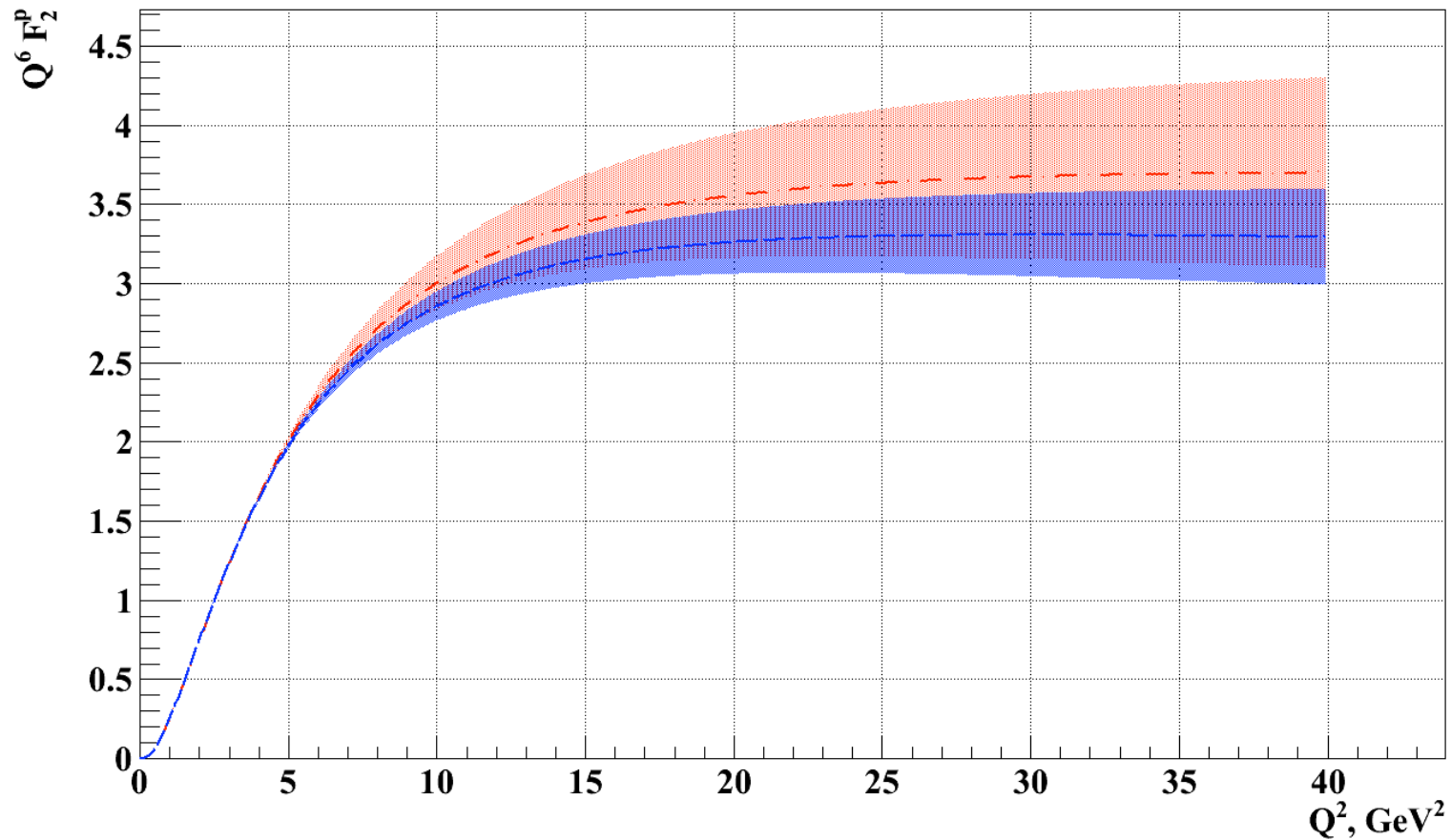
# Global Fit and $G_M^p$



- Global analysis using constraint on R from polarization data brings a small systematic increase in  $G_M^p$ , consistent with Brash 2001 and Arrington, Melnitchouk, Tjon 2007 (TPEX effects neglected in our analysis), due to smaller  $G_E^{p2}$  contribution to  $\sigma_r$ .

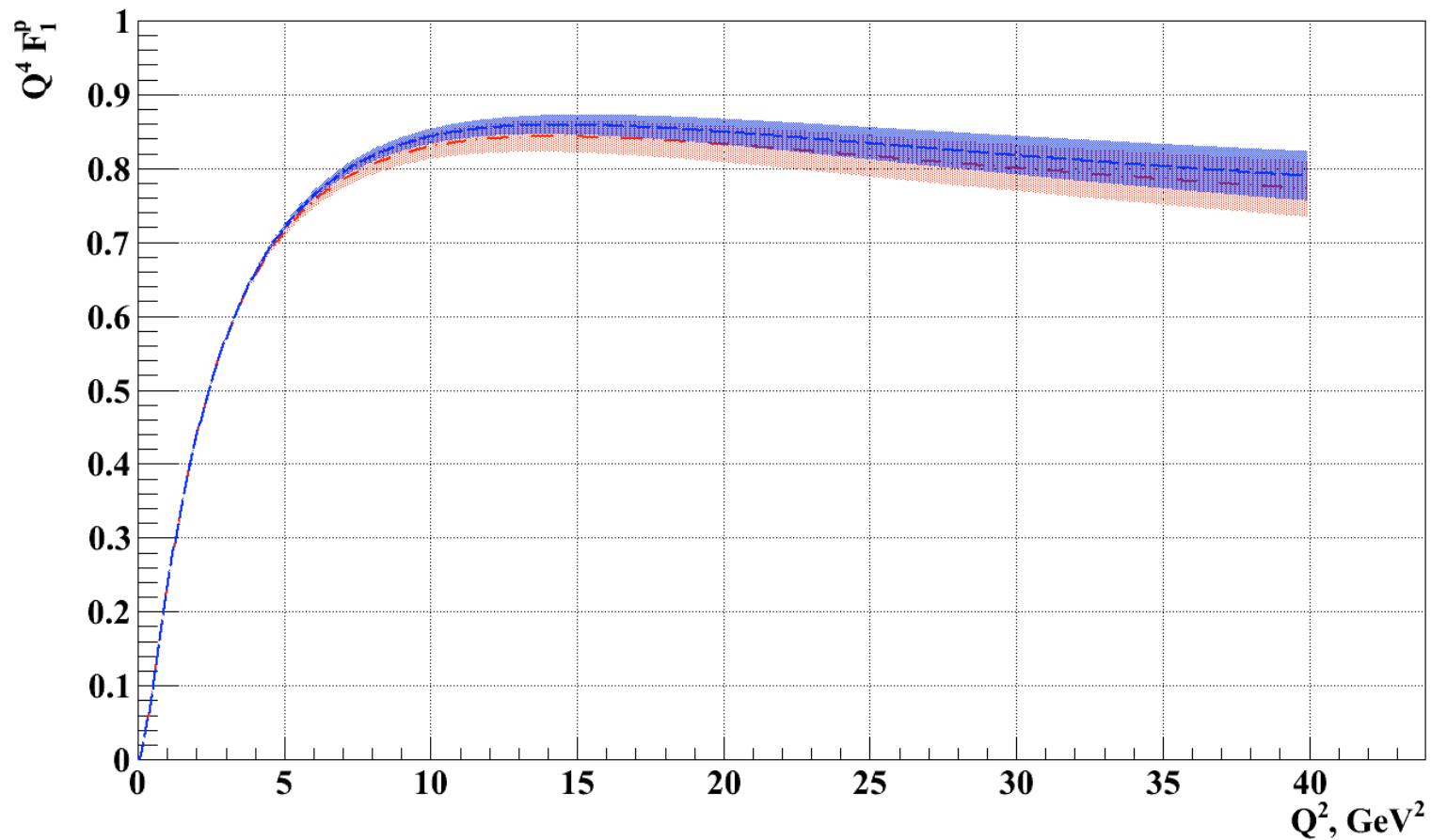


# Global Fit and $F_2^p$



Global fit of  $Q^6 F_2^p$  **before/after** GEp-III

# Global Fit and $F_1^p$



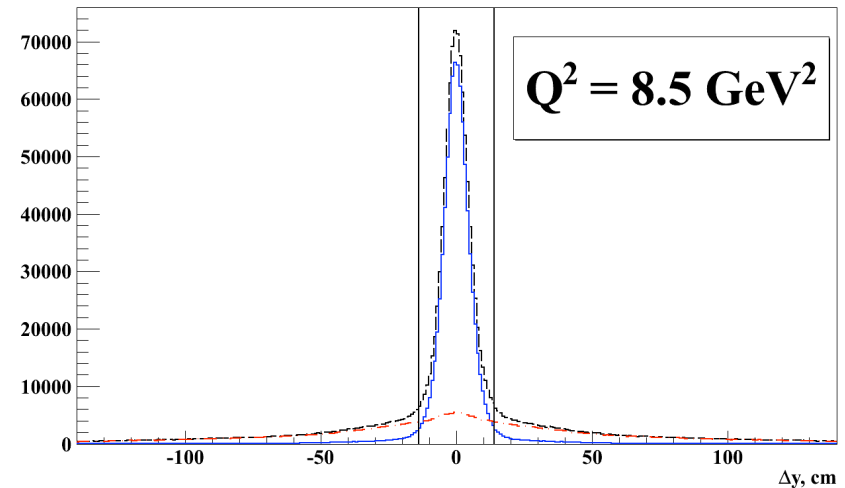
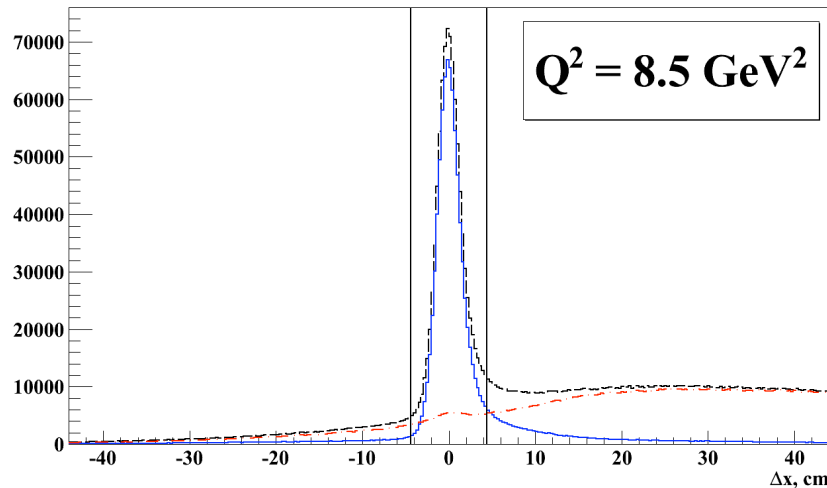
Global fit of  $Q^4 F_1^p$ , **before/after** GEp-III

# Conclusion

- GEp-III results finalized, accepted for publication in PRL
- Extended recoil polarization data to  $Q^2 = 8.5$  GeV<sup>2</sup>
- Significant new constraints on high- $Q^2$  behavior of F. F. models, GPD moments, transverse charge and magnetization densities, etc.
- GEp-2 $\gamma$  results not far behind!

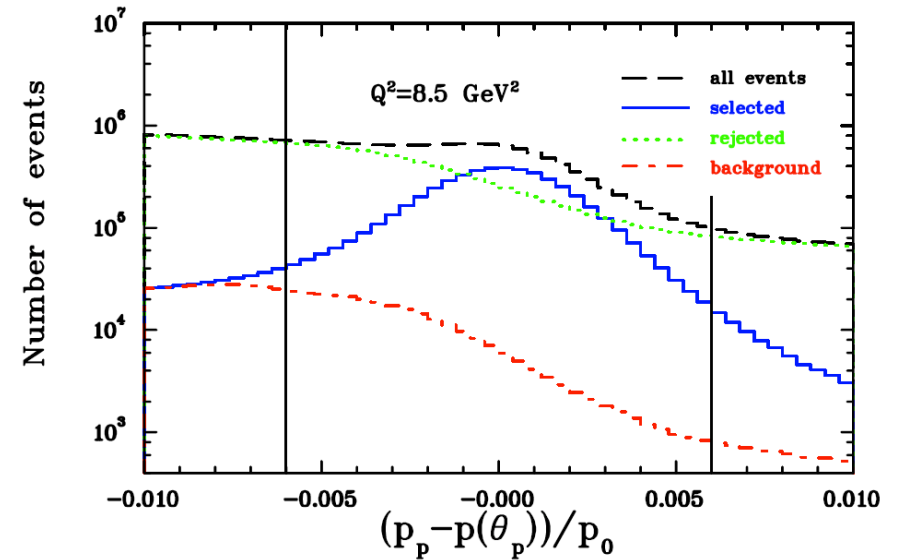
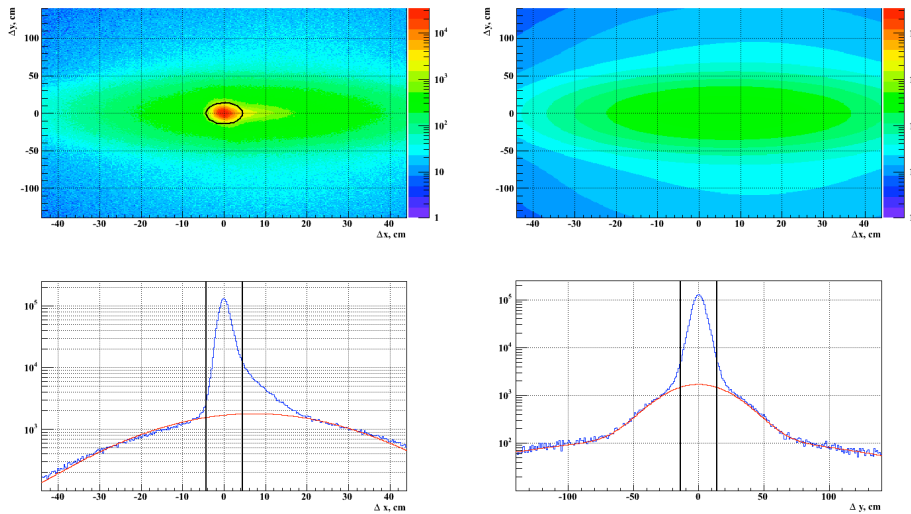
# Backup Slides

# Elastic Event Selection

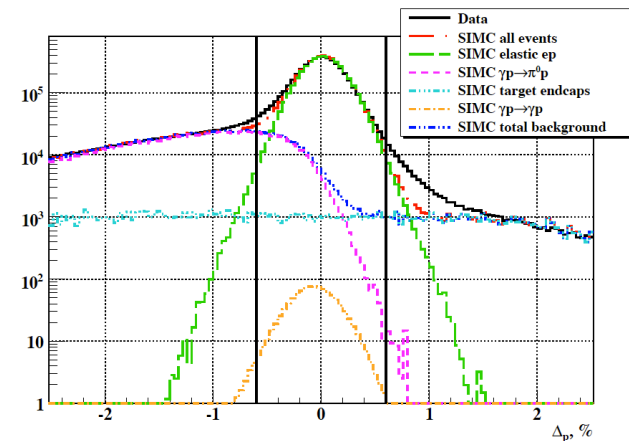


- Electron coordinates/angles + proton momentum measured with excellent resolution; use these quantities to define cut variables
- Calculate  $\theta_e$  from  $E_e$ ,  $p_p$
- Calculate  $\varphi_e$  from  $\varphi_p$  (coplanarity)
- Project from vertex to BigCal, compare to measured electron coordinates
- Above: projections of horizontal (dx) and vertical (dy) coordinate differences:
  - **No cut,  $3\sigma$  dp cut,  $3\sigma$  dp anticut**
  - Tight dp cut rejects some small fraction of elastic events (small “bumps”)

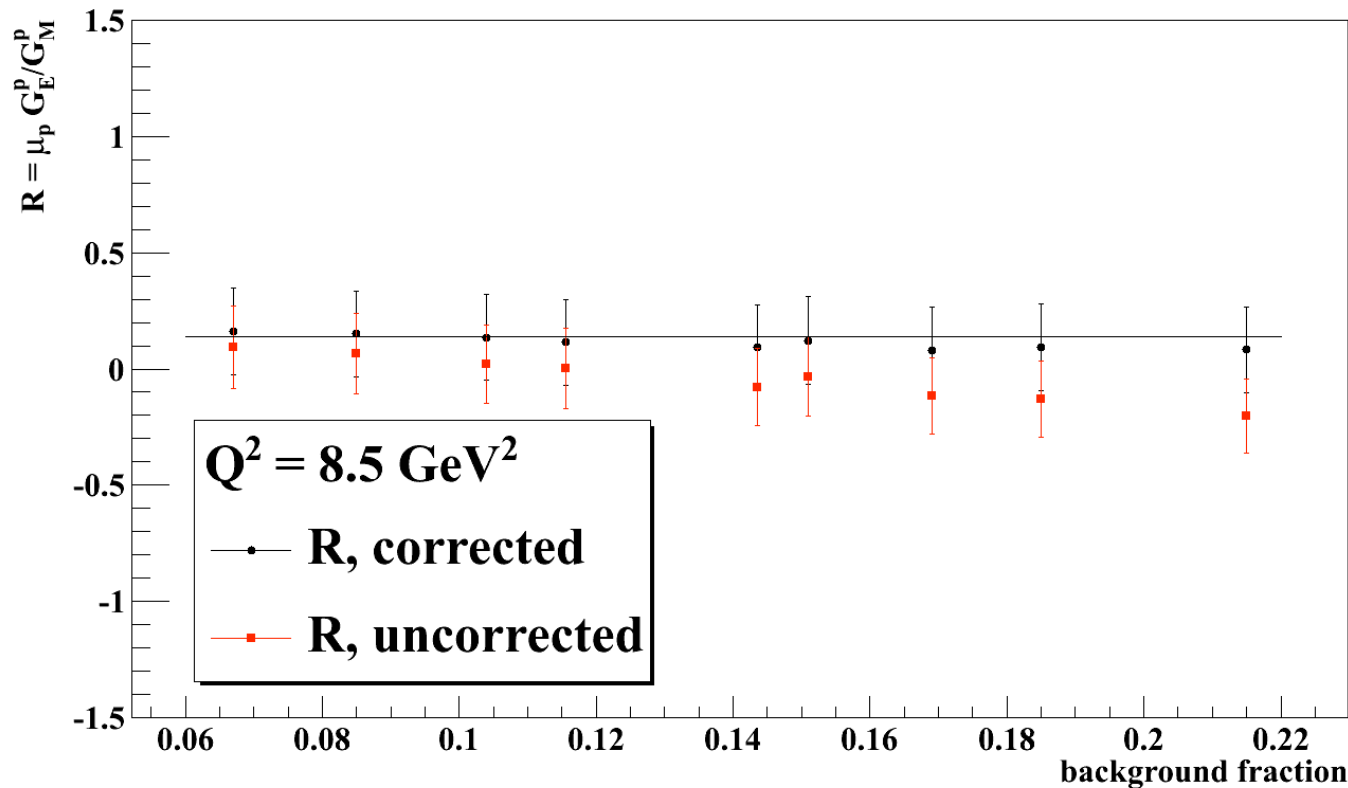
# Background Estimation



- Estimate background directly from data by extrapolating dx, dy distribution under the peak (above):
  - Data, fitted background and projections
- Compare data (top right) and MC (bottom right) for dp



# Background Subtraction



$$f = \frac{N_{inel.}}{N_{el.} + N_{inel.}}$$

$$P_{obs} = (1 - f)P_{el} + fP_{inel}$$

$$P_{el} = \frac{P_{obs} - fP_{inel}}{(1 - f)}$$

- Background and signal polarizations differ, F. F. ratio decreases as elastic cuts are relaxed
- Stability of background-subtracted F. F. ratio w.r.t. cut variations including more background validates background subtraction method

# Extraction of Polarization Observables

$$N^\pm(\vartheta, \varphi) = N_0^\pm \frac{\varepsilon(\vartheta)}{2\pi} \left[ \begin{array}{l} 1 + (c_1(\vartheta) \pm A_y(\vartheta) P_y^{fpp}) \cos \varphi \\ + (s_1(\vartheta) \mp A_y(\vartheta) P_x^{fpp}) \sin \varphi + \\ c_2(\vartheta) \cos(2\varphi) + s_2(\vartheta) \sin(2\varphi) + \dots \end{array} \right]$$

$$f_\pm = \frac{N^\pm(\vartheta, \varphi)}{N_0^\pm}$$

$$f_+ + f_- = \frac{\varepsilon(\vartheta)}{\pi} \left[ \begin{array}{l} 1 + c_1 \cos \varphi + s_1 \sin \varphi + \\ c_2 \cos(2\varphi) + s_2 \sin(2\varphi) + \dots \end{array} \right]$$

$$f_+ - f_- = \frac{\varepsilon(\vartheta) A_y(\vartheta)}{\pi} \left[ P_y^{fpp} \cos \varphi - P_x^{fpp} \sin \varphi \right]$$

Angular distribution and azimuthal asymmetry definitions



# Spin Precession, I

$$\frac{d\vec{S}}{dt} = \frac{e}{m\gamma} \vec{S} \times \left[ \frac{g}{2} \vec{B}_{\parallel} + \left( 1 + \gamma \left( \frac{g}{2} - 1 \right) \right) \vec{B}_{\perp} \right]$$

$$\frac{d\vec{v}}{dt} = \frac{e}{m\gamma} \vec{v} \times \vec{B}$$

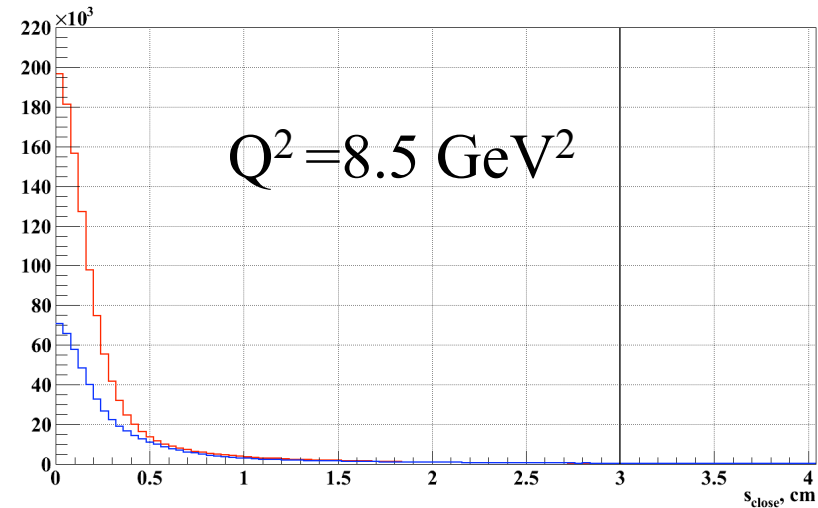
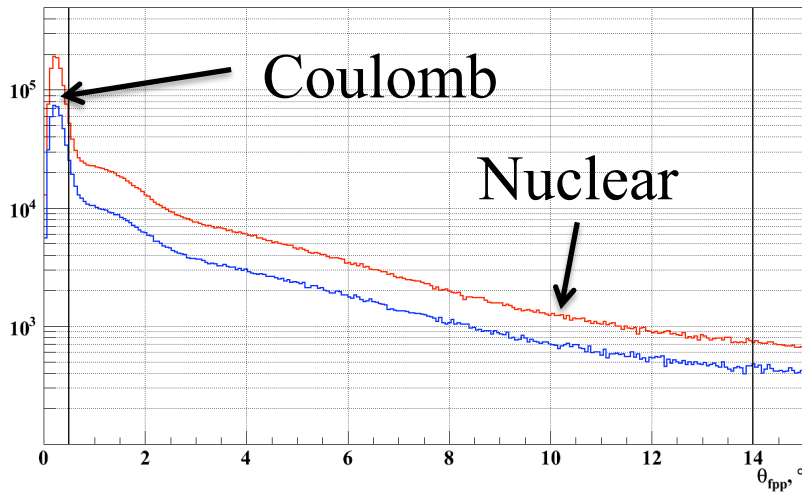
$$\left( \frac{d\vec{S}}{dt} \right)_{\text{comoving}} \xrightarrow{B_{\parallel}=0} \gamma \left( \frac{g}{2} - 1 \right) \frac{e}{m\gamma} \vec{S} \times \vec{B}$$

$$\chi = \gamma \kappa \theta_{\text{bend}}$$

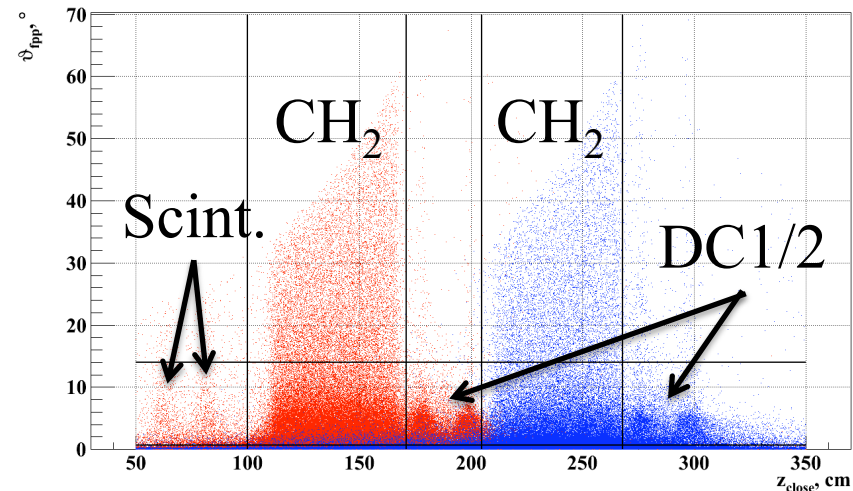
$Q^2, \text{ GeV}^2$	$p_0, \text{ GeV}/c$	$\chi_{\theta}, ^{\circ}$
2.5	2.0676	108.5
5.2	3.5887	177.2
6.7	4.4644	217.9
8.5	5.4070	262.2

- BMT equation (1959): relativistic spin precession in a magnetic field
- $\chi$  = precession angle relative to velocity in a constant, uniform magnetic field
- Precession angles corresponding to HMS 25° central bend for this experiment shown in table
- Unique spin rotation for each event, calculated using HMS COSY model

# FPP Reconstruction

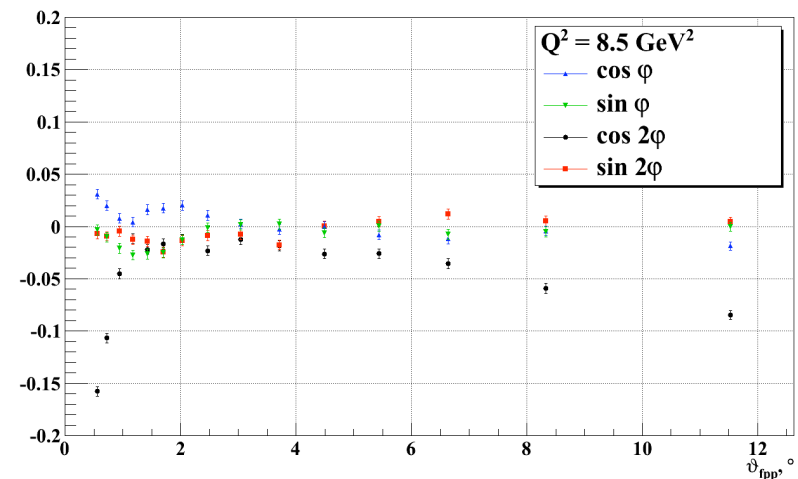
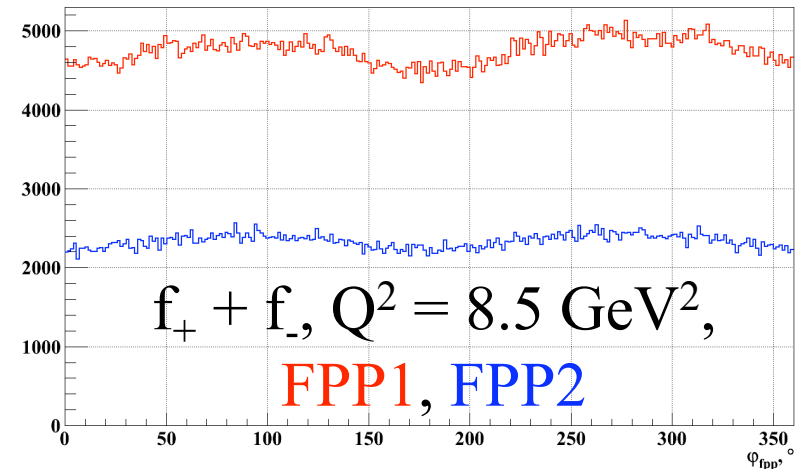


- **FPP1** (**FPP2**) event distributions:
  - Polar angle  $\theta$  (top left)
  - Closest approach distance  $s_{\text{close}}$  (top right)
  - $\theta$  vs point of closest approach  $z_{\text{close}}$  (bottom right)
- Black lines represent analysis cuts

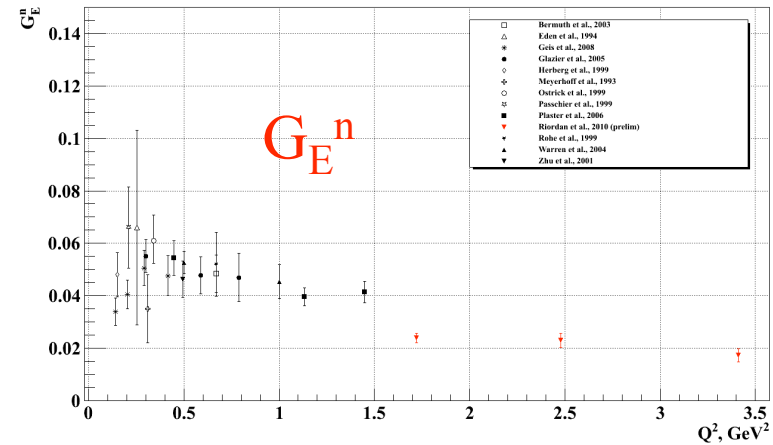
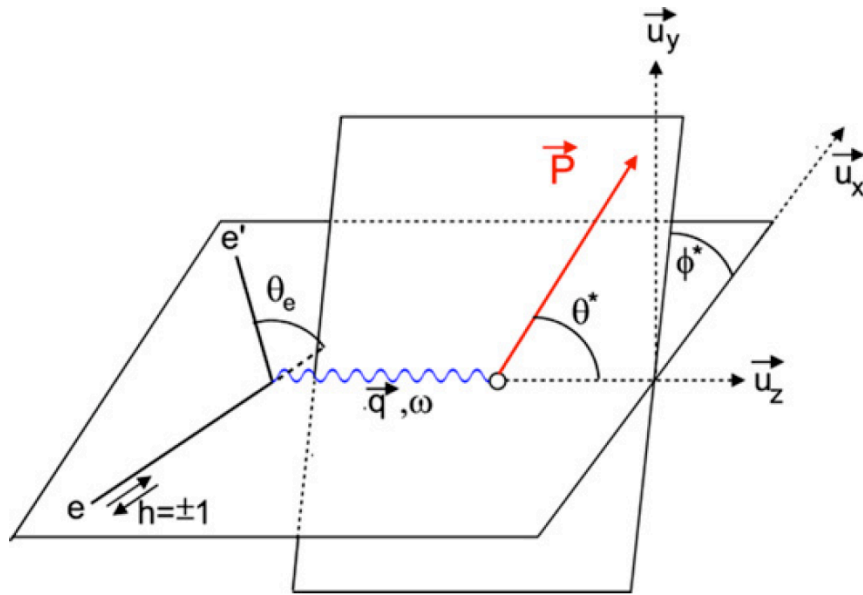


# False Asymmetries

- Helicity-independent false/instrumental asymmetries caused by:
  - FPP acceptance/efficiency
  - $\phi$  misreconstruction:
    - Misalignment ( $1\phi$ )
    - xy resolution asymmetry ( $2\phi$ )
- $\theta$ -dependent (bottom right)
- Cancelled by helicity reversal to first order
- Second-order effects small
- *Measured* using sum distribution and *corrected* in analysis

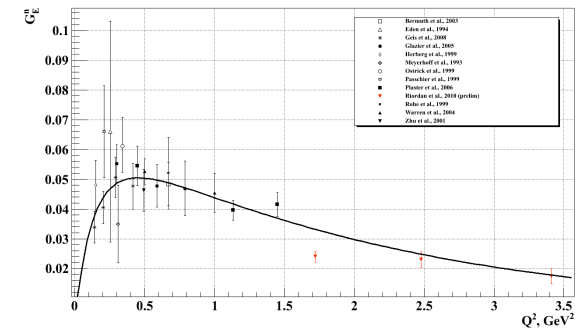
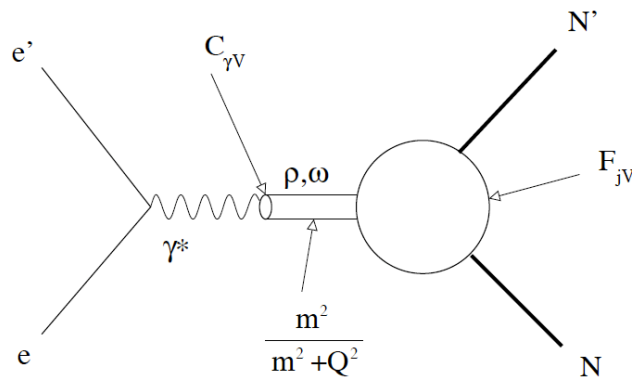
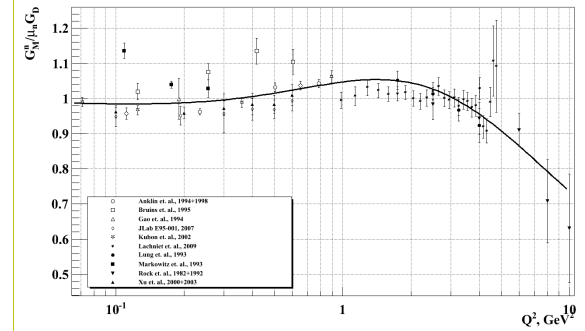
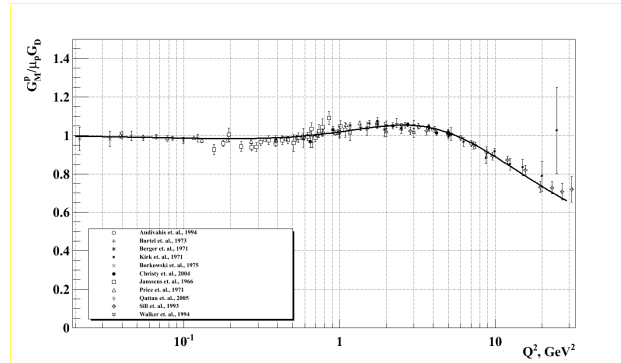
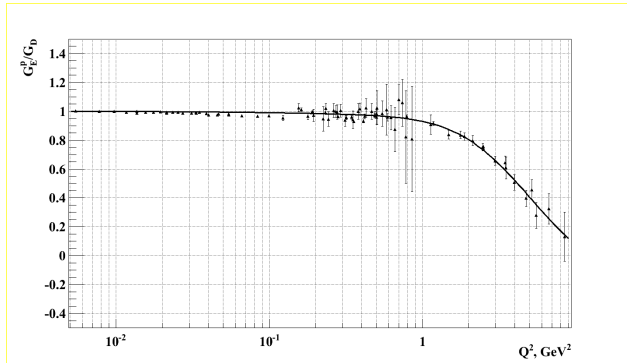


# Polarized Target Asymmetry and $G_E^n$



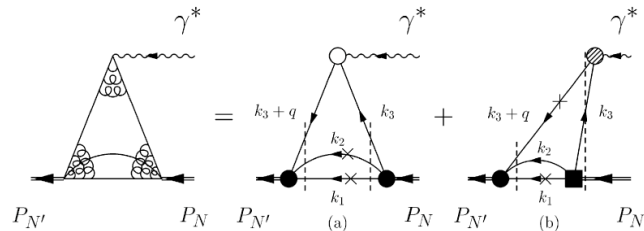
- Polarized beam on polarized target
- Beam helicity asymmetry sensitive to  $G_E/G_M$
- Maximal sensitivity for target polarization perp. to  $q$  in scattering plane
- Nearly all  $G_E^n$  data obtained from:
 
$${}^3\vec{He}(\vec{e}, e' n), {}^3\vec{He}(\vec{e}, e'), {}^2H(\vec{e}, e' \vec{n})$$

# VMD

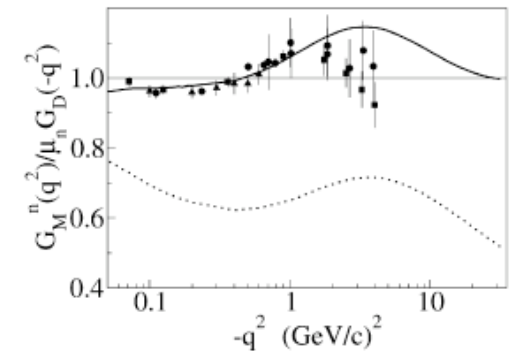
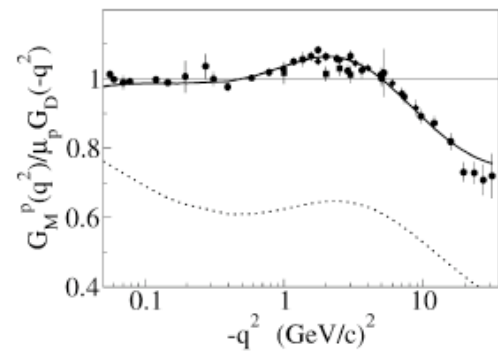
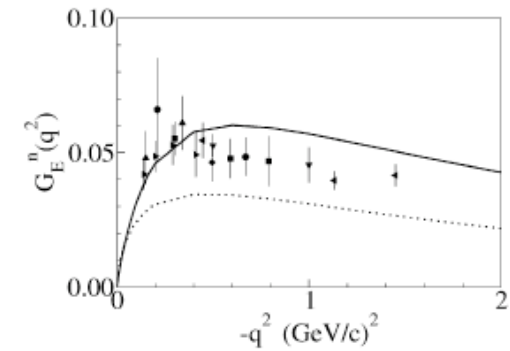
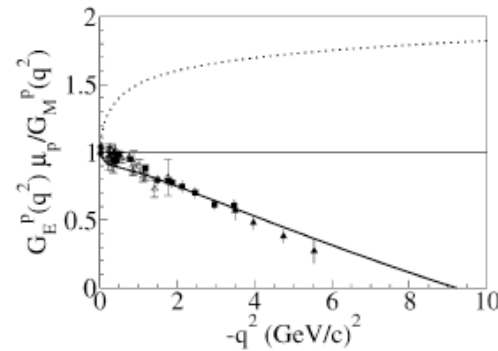


- Fits by Lomon in extended Gari-Krumpelmann model, nucl-th/0609020
- $\rho$ ,  $\omega$ ,  $\phi$ ,  $\rho'$ ,  $\omega'$  mesons + “direct coupling” enforces pQCD asymptotic behavior

# Bethe-Salpeter Amplitude

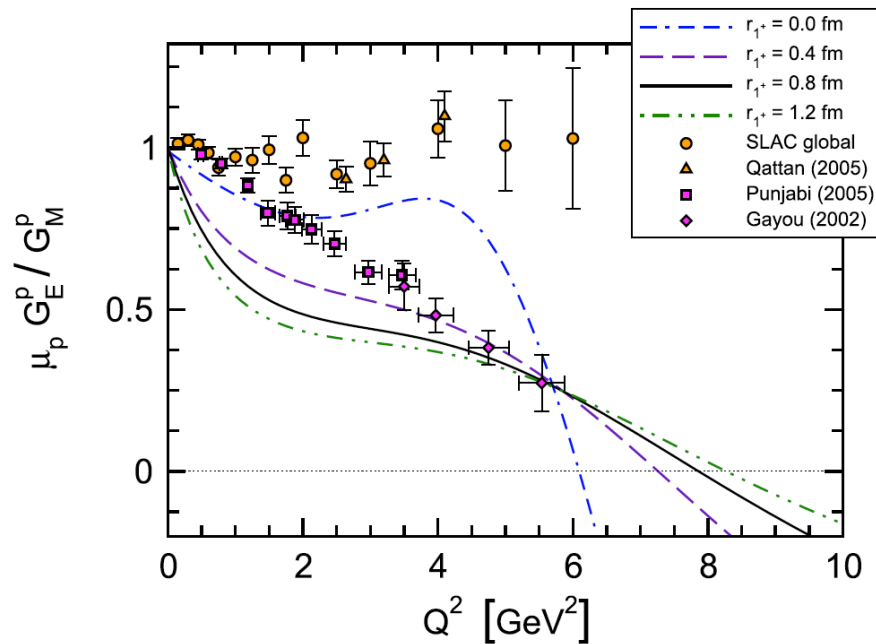


Combined Ansatz for nucleon Bethe-Salpeter amplitude and microscopic VMD model, consider valence and non-valence components of the nucleon state in light-front dynamics



de Melo et al. PLB 671, 153 (2009)

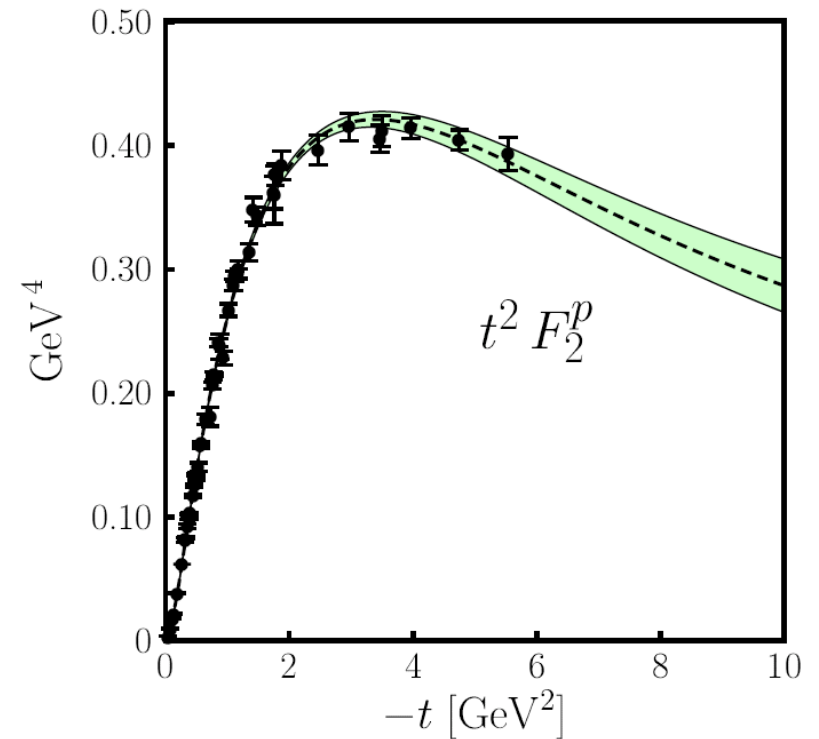
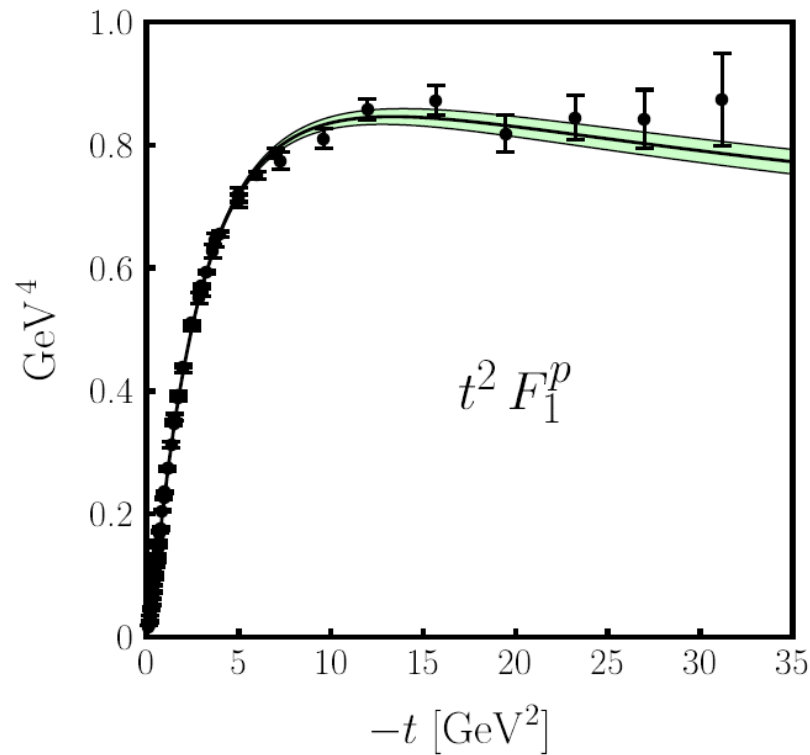
# Dyson-Schwinger/Faddeev/q(qq)



Dressed-quark core contribution to  $R_p$  for different diquark radii

- Cloet et al., Few Body Systems, 46, 1 (2009)
- Dressed quarks are fundamental degrees of freedom
- diquark correlations
- Solution of Poincare-covariant Faddeev equations based on rainbow-ladder truncation of DSEs of QCD
- photon-nucleon vertex depends on a single parameter: diquark charge radius
- $G_{Ep}$  and  $G_{En}$  both possess a zero

# GPDs, I



$$\int_{-1}^1 dx H^q(x, \xi, t) = F_1^q(t)$$

$$\int_{-1}^1 dx E^q(x, \xi, t) = F_2^q(t)$$

- Form factors constrain GPDs through sum rules: 0<sup>th</sup> moments of vector (H) and tensor (E) GPDs equal e.m. form factors
- Above: Diehl et al; EPJ C, 39, 1 (2005)

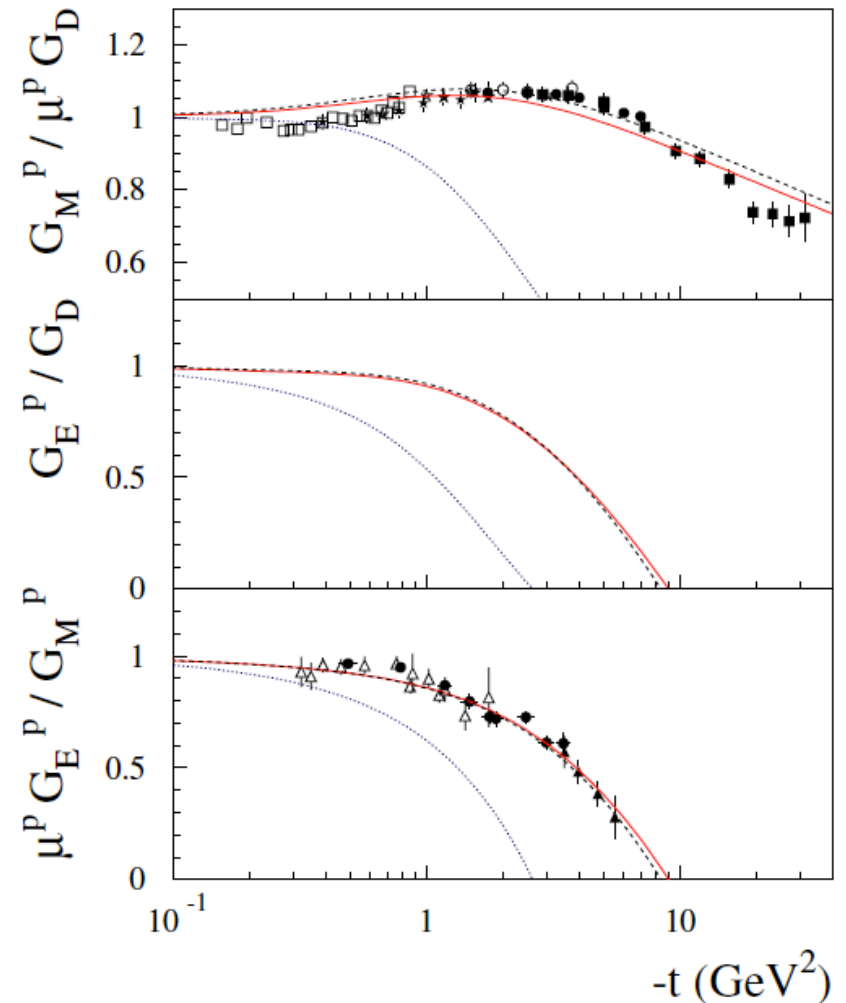


# GPDs, II

- Guidal et al., PRD 72, 054013  
2005: Modified Regge parametrization of valence quark GPDs
- Three-parameter fit to nucleon form factor data
- Constraint on E from precise  $F_{2p}$  data allowed evaluation of Ji sum rule:

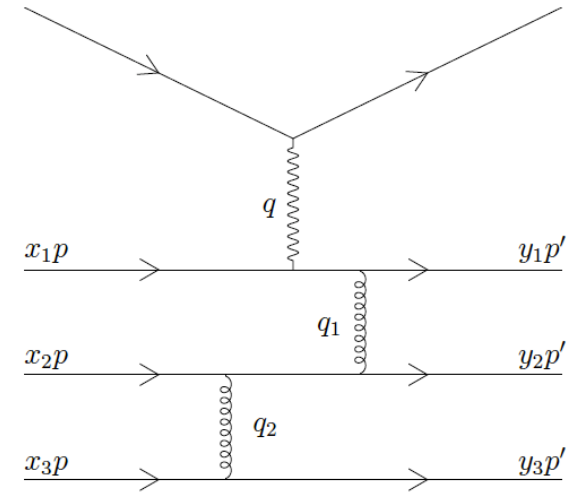
$$2J^q = \int_{-1}^1 dx x \{H^q(x, 0, 0) + E^q(x, 0, 0)\},$$

	$M_2^q$ (MRST2002)	$2J^q$ (R2 model)	$2J^q$ (lattice [40])
$u$	0.37	0.58	$0.74 \pm 0.12$
$d$	0.20	-0.06	$-0.08 \pm 0.08$
$s$	0.04	0.04	
$u + d + s$	0.61	0.56	$0.66 \pm 0.14$

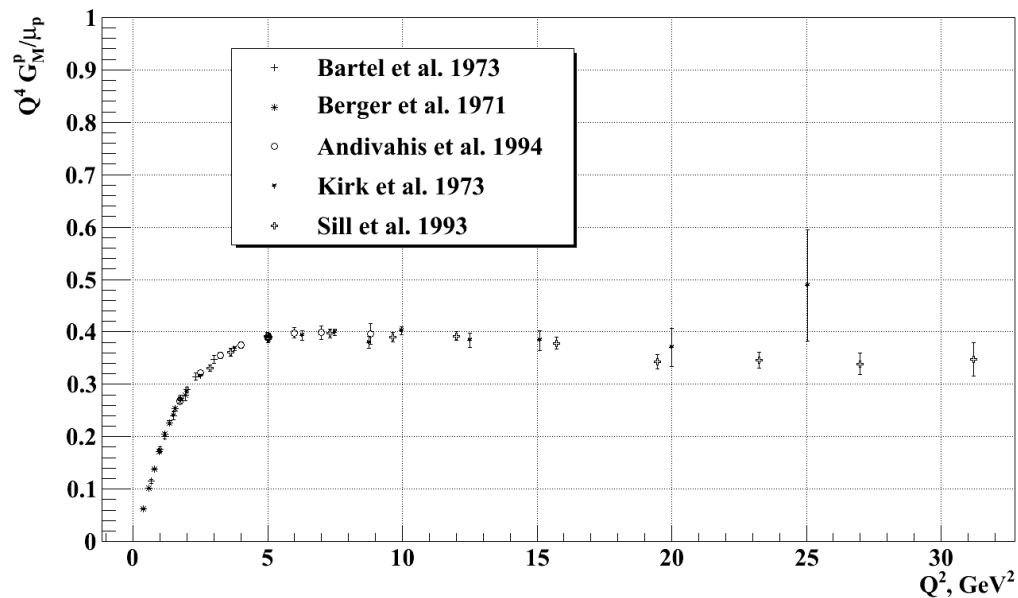


# pQCD, I

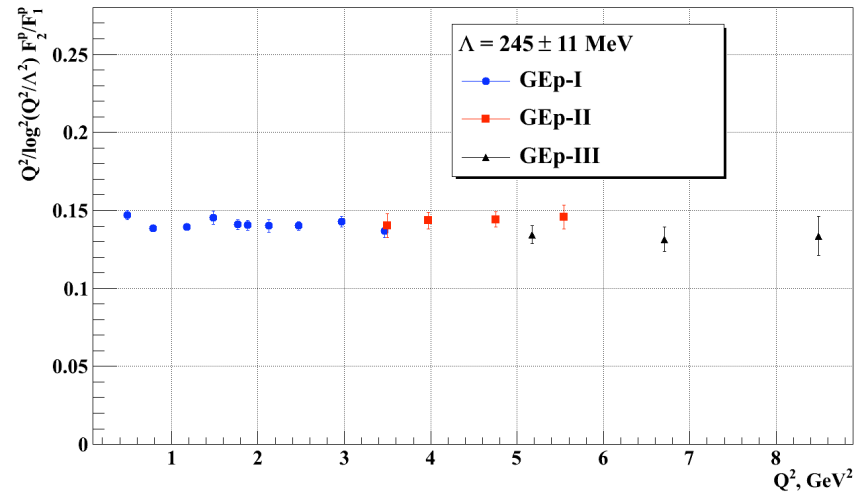
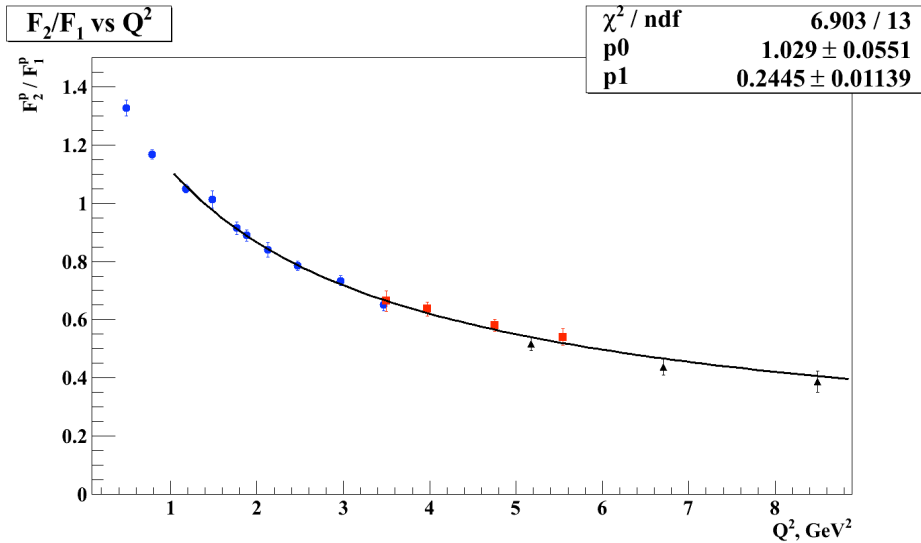
- Based on dimensional scaling laws for high- $Q^2$  exclusive reactions:
  - Brodsky, Farrar, PRD 11, 1309 (1975)
  - Brodsky, Lepage PRL 43, 545 (1979)
- Expect  $F_{1p} \sim 1/Q^4$ ,  $F_{2p} \sim 1/Q^6$ , as  $Q^2 \rightarrow \infty$



Approximately satisfied by  
 $G_{Mp}$  starting at  $Q^2 \approx 5-10$   
 $\text{GeV}^2$



# pQCD, II

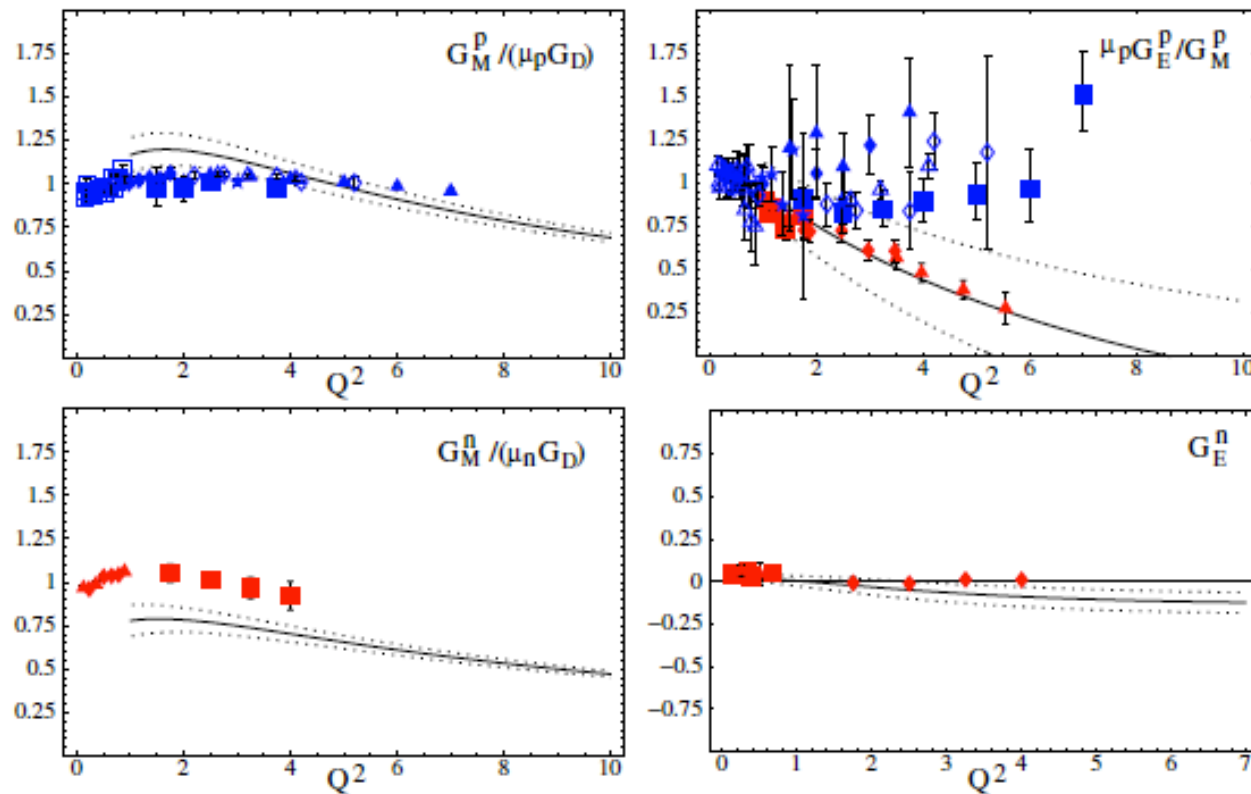


- Belitsky, Ji, Yuan, PRL 91, 092003 (2003)
- pQCD analysis of Pauli form factor  $F_2$
- Subleading-twist component of light cone nucleon D. A. leads to logarithmic modification of asymptotic scaling of  $F_2$  relative to  $F_1$

- Proton data for the *ratio*  $F_2/F_1$  well described by this modified scaling
- Necessary, but not sufficient condition for validity of pQCD form factor description

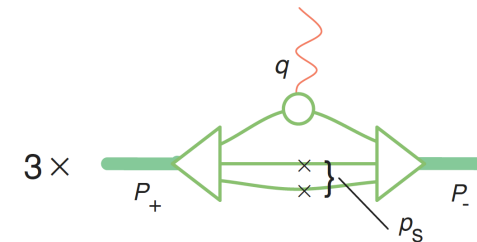
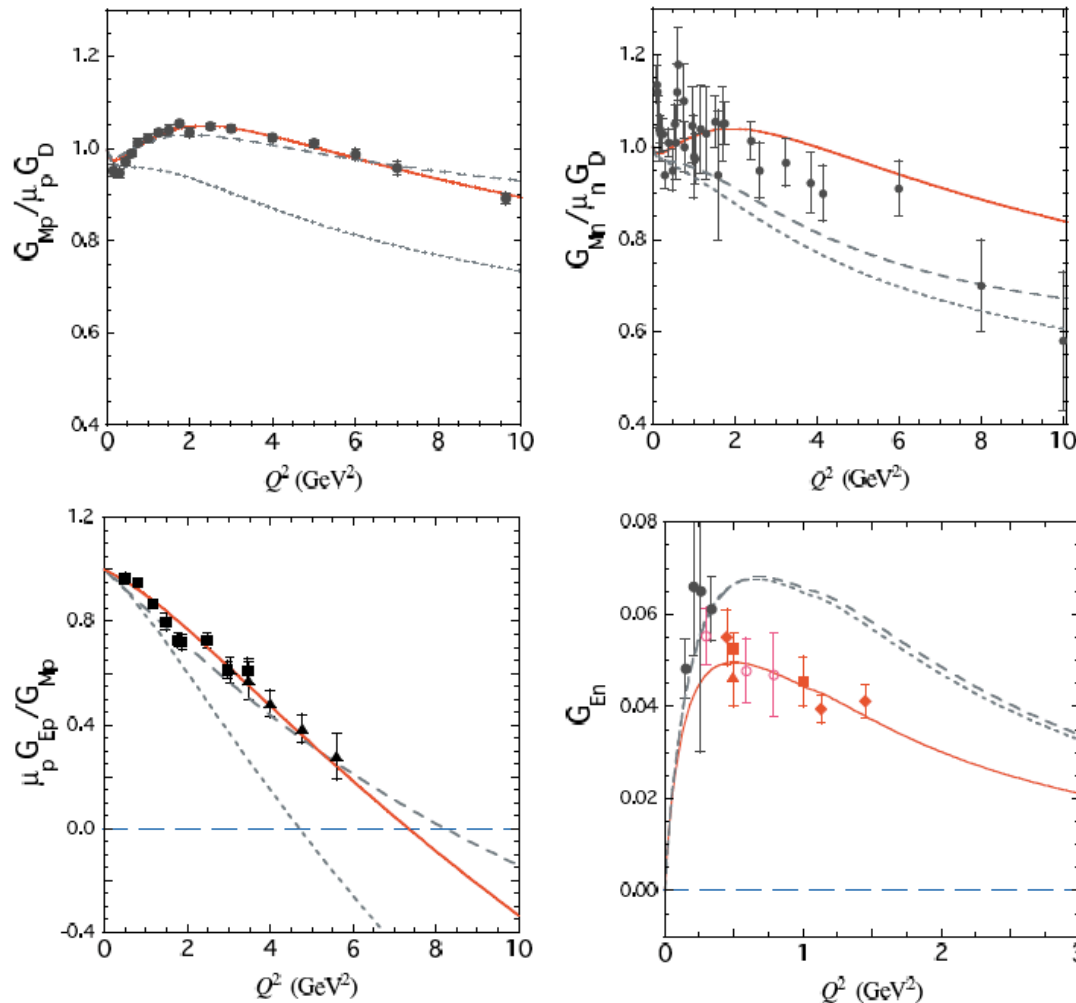
$$Q^2 \frac{F_2}{F_1} \propto \ln^2 \left( \frac{Q^2}{\Lambda^2} \right)$$

# pQCD, III



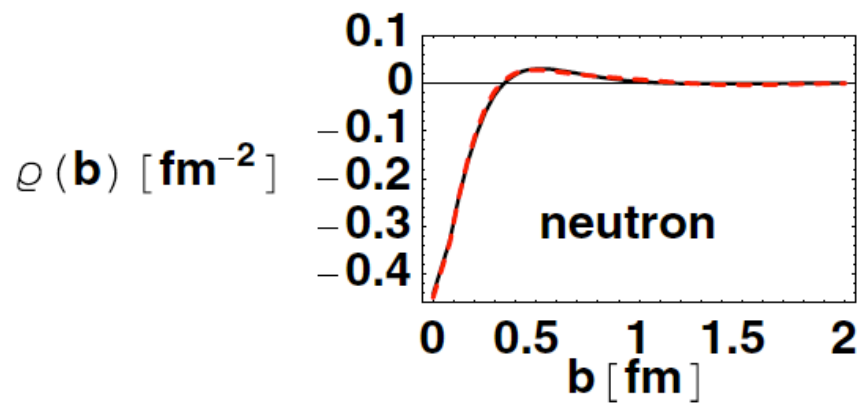
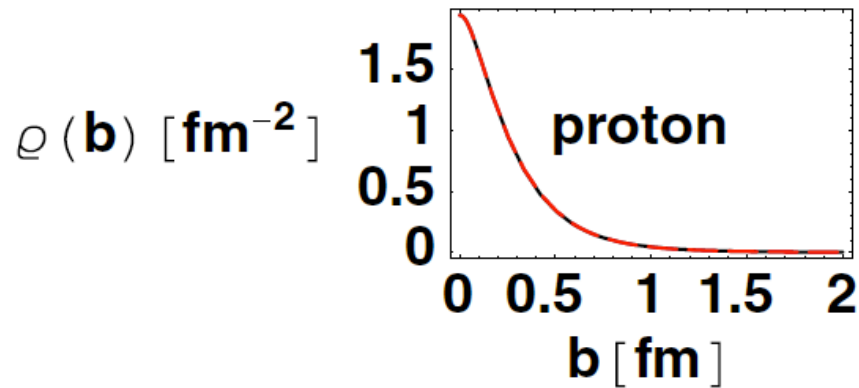
Light cone QCD sum rule calculation of nucleon form factors: Braun, Lenz, and Wittmann, PRD 73, 094019 (2006)

# Covariant Spectator Model



- Gross and Agbakpe, PRC 73, 015203 (2006)
- Model nucleon as bound state of three dressed, valence constituent quarks
- Covariant spectator “diquark” on shell

# Transverse Densities



- Burkardt, Int. J. Mod. Phys. A 18, 173 (2003)—GPDs related to impact-parameter distributions:

$$q(x, \mathbf{b}) = \int \frac{d^2 q}{(2\pi)^2} e^{i\mathbf{q}\cdot\mathbf{b}} H_q(x, t = -\mathbf{q}^2),$$

- Miller, PRL 99, 112001 (2007)—model-independent transverse charge density from 2D Fourier transform of  $F_{1p}$
- Miller, Piassetzky, Ron, PRL 101, 082002 (2008)—model-independent magnetization density from  $F_{2p}$

$$\rho(b) \equiv \sum_q e_q \int dx q(x, \mathbf{b}) = \int \frac{d^2 q}{(2\pi)^2} F_1(Q^2 = \mathbf{q}^2) e^{i\mathbf{q}\cdot\mathbf{b}}. \quad \rho_M(b) = \int \frac{d^2 q}{(2\pi)^2} F_2(t = -\mathbf{q}^2) e^{i\mathbf{q}\cdot\mathbf{b}}.$$